Hardcastle IR.

Protein-protein interaction inhibitors.

***In:* Bernstein, P.R.; Georg, G.I.; Keller, Th.; Kobayashi, T.; Lowe, J.A.; Meanwell, N.A.; Saxena, A.K.; Stilz, U.; Supuran, C.T.; Zhang, A, ed. *Topics in Medicinal Chemistry*. Berlin, Heidelberg: Springer, 2017,**

https://doi.org/10.1007/7355_2017_27

Abbreviations

acute lymphoblastic leukaemia (ALL)
B-cell lymphoma 2 (Bcl-2)
B-cell lymphoma/leukemia 11B protein (Bcl-B)
B-cell lymphoma-extra large (Bcl-xL)
Bcl-2-associated death promoter (Bad)
Bcl-2-associated protein (Bax)
Bcl-2-homologous antagonist killer (Bak)
Bcl-2-like protein 2 (Bcl-w)
BH3 interacting-domain death agonist (Bid)
Chronic lymphocytic leukemia (CLL)
induced myeloid leukemia cell differentiation protein (Mcl-1)
mammalian target of rapamycin protein (mTOR)
mouse double minute 2 (MDM2)
NF-kappa-B-inducing kinase (NIK)
Nuclear Factor-kappa-B (NF-κB)
p53 upregulated modulator of apoptosis (PUMA)
Receptor-interacting serine/threonine-protein kinase 1 (RIPK1)
small cell lung cancer (SCLC)
second mitochondria-derived activator of caspases (Smac)
small lymphocytic leukemia (SLL)
truncated BH3 interacting-domain death agonist (t-Bid)
TNF-related apoptosis-inducing ligand (TRAIL)
X-linked inhibitor of apoptosis protein (XIAP)

Protein-protein interaction inhibitors

Ian Robert Hardcastle

Ian.Hardcastle@ncl.ac.uk

Newcastle Cancer Centre at the Northern Institute for Cancer Research
School of Chemistry
Bedson Building
Newcastle University
NE1 7RU

+44 191 208 6645

Abstract

The study of cellular mechanisms of cancer growth and survival has revealed a complex web of signalling pathways that produce the 'hallmarks of cancer'. A number of critical cellular signalling nodes have been characterised from which many new drug targets have been proposed. A number of these nodes are regulated by protein-protein interactions, and so present attractive, if challenging, targets for drug discovery. Drug discovery efforts towards three PPI families have resulted in clinically investigated drugs: i.e. Bcl-2 family inhibitors, MDM2-p53 inhibitors and IAP inhibitors. The discovery and optimisation of these drug classes are detailed in this chapter.

PPI targets in cancer

The modern understanding of cancer biology is that tumour cells have acquired the characteristic 'hallmarks of cancer' through gain-of-function mutations to oncogenes and loss-of-function of tumour suppressor genes.[1] Detailed examination of signalling pathways associated with hallmark traits has allowed the identification of numerous potential targets for intervention by therapeutic agents, in many cases with small-molecule drugs. A number of the pathways investigated thus far rely on signalling *via* nodes regulated by protein-protein interactions (PPIs). In particular, PPIs regulating the apoptotic response of a cell have been characterised, providing promising areas for drug discovery, for example, between members of the B-cell lymphoma 2 (Bcl-2) family, the mouse double minute 2 (MDM2)-p53 interaction, and the interaction of second mitochondria-derived activator of caspases protein with X-linked inhibitor of apoptosis protein (Smac-XIAP). This chapter will describe each of these PPI targets and the discovery of small-molecule PPI inhibitor drugs that have entered clinical trials.

PPI chemotherapy drugs

Historically, extensive screening of natural products was used to identify compounds with cytotoxic activity for use in chemotherapy regimens. For a number of compounds investigated, the molecular mechanism of action was identified to be the disruption of a PPI (Table 1).

The regulation of microtubule cycling by the polymerisation and depolymerisation of α,β-tubulin, is essential for the organisation of DNA during the M-phase of the cell cycle, and is targeted by a number of natural products from diverse sources. Isolated from plant sources, the vinca alkaloids e.g. vinblastine (**1**), and the taxoids e.g. taxol (**2**) were initially thought to share the same mechanism of action. However, detailed studies indicated that vinblastine (**1**) acts by binding into a hydrophobic groove at the interface of the α- and β-tubulin subunits at the ends of microtubules, and stabilises the microtubule at low concentrations, but induces depolymerisation at higher concentrations.[2] In contrast, taxol (**2**) binds to the β-tubulin subunit close to the GTP-binding site.[3–5] A conformational change is induced by drug binding that results in an unusually strong interaction between subunits and consequently microtubules grow in an uncontrolled manner. Isolated from marine sponges, the natural product Halichondrin B (**3**) and the simplified synthetic derivative Erubilin (**4**) also bind to microtubules close to the vinca binding site, and overlapping with the GTP-binding site, suppressing the growth of microtubules.[6,7] Isolated from the myxobacteria *Sorangium cellulosum*, Epothilones e.g. **5** have a similar mechanism of action as the taxoids, and promote microtubule growth.

The semi-synthetic derivative of rapamycin, temsirolimus (**6**) inhibits the kinase activity of the mammalian target of rapamycin protein (mTOR) by forming a protein-protein complex with the FK506 binding protein 12 (FKBP12).[8]

Druggability of PPIs

Despite the serendipitous discovery of PPIs as cancer therapies, until recently the established view from medicinal chemists has been that PPI targets are significantly less 'druggable' than enzyme or receptor targets. The reasoning for this is based on the high surface area for PPI targets (1500 – 4660 Å^2) compared with other drug-protein interfaces (1200 - 2000 Å^2), and their relatively high binding affinities (ΔG = -7.0 to -17.2 kcal/mol).[9] Other analyses suggested that PPIs are more circular, flatter, less polar, and present fewer opportunities for H-bonding than enzyme or receptor drug targets.[10] The negative outlook from these global analyses of PPIs, has been contradicted by detailed investigations of PPI binding sites, including alanine-scanning mutagenesis, that have revealed that many PPIs include small regions of high binding affinity called 'hot-spots' that can have attractive features for small molecule binding.[11,12] Hot-spots may include the binding sites for large amino acid side chains on one protein that bind to small pockets on the partner protein, and may be circled by polar residues.[13] 'Hot segments' are larger continuous epitopes that contribute the majority of the binding energy of a PPI.[14] The most tractable of these for drug discovery are the interactions between a continuous peptide sequence of one peptide that interacts with a defined domain of the partner protein. The interfaces between protein and α-helical epitopes have demonstrated good tractability as drug targets, as exemplified by the development of Bcl-2 family and MDM2-p53 PPI inhibitors (*vide infra*).

Targeting PPIs with small-molecules may have some advantages as they represent an under exploited class within the 'druggable genome' and may present opportunities to inhibit cellular pathways that would be difficult to approach though other target classes.[15] PPIs may offer better opportunities for selectivity in comparison to competitive inhibition of enzymes at their substrate of co-factor binding sites due to the size and structural diversity of the interactions targeted. Unfortunately, the proposal that PPI inhibitors will offer a lower likelihood of developing resistance has not been borne out in clinical experience, especially in the case of MDM2-p53 inhibitors.[16,17]

Bcl family inhibitors

Biology

The response of cells to a variety of signals resulting in programmed cell death or apoptosis is controlled by the PPIs of a family of proteins related to Bcl-2.[18,19] Within the family, proteins can be grouped according to their role (Figure 1). The BH3-only proteins (e.g. Bcl-2-associated death promoter (Bad) and p53 upregulated modulator of apoptosis (PUMA)) act as initiators of apoptosis in response to cytokine deprivation, intracellular damage or oncogenic signalling, whereas truncated BH3 interacting-domain death agonist (t-Bid) is activated by the death receptor and signalling via caspase 8. Activation of BH3 proteins induces the negative regulation of the pro-survival Bcl-2 proteins, and activation of the pro-apoptotic effector proteins, either Bcl-2-associated protein (Bax) or Bcl-2-homologous antagonist killer (Bak), which disrupt the outer membrane of mitochondria and initiate the apoptotic cascade.

Given the pivotal role of the Bcl-2 proteins in regulating cell death, it is not surprising that dysregulation of the pathway is strongly linked to the development of cancer. Overexpression of pro-survival proteins is linked to tumours, e.g. Bcl-2 overexpression is found in 90% of follicular centre B cell lymphomas,[20] and *MCL-1* or *BCL2L1* are amplified in a variety of tumours.[21] Similarly, deletion or downregulation of BH3 initiator genes, *BIM* and *PUMA* has been observed in tumours.[22–24] Abnormalities in the Bcl-2 pathway are also associated with resistance to chemotherapy and radiotherapy.[25]

The prospect of activating apoptosis in tumour cells where the Bcl-2 pathway is defective provides an attractive approach to new cancer therapies. Compounds have been sought that mimic the action of pro-apoptotic BH3 proteins by binding to Bcl-2 family members to block their pro-survival action and so induce apoptosis directly.

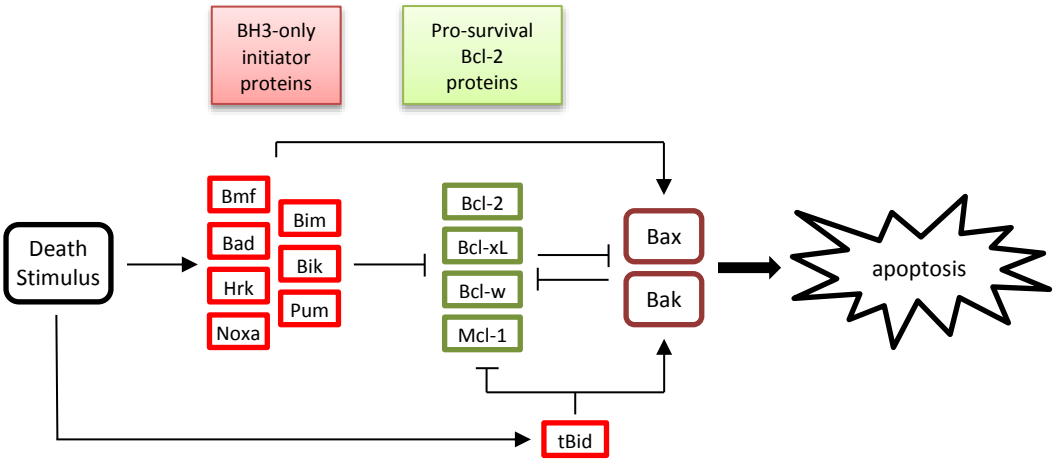

Figure 1: Apoptotic signalling via the Bcl-family proteins.

Structural biology and peptides

NMR and X-ray studies with the B-cell lymphoma-extra large (Bcl-xL) protein provided a structural understanding of the domains involved in the anti- and pro-apoptotic activity of the protein.[26] The tBH1, BH2 and BH3 domains of Bcl-xL form a hydrophobic cleft, which is the site for interactions with the pro-death proteins, Bax and Bak. The NMR solution structure of Bcl-xL bound to a Bak BH3 domain peptide shows the Bak peptide forms an amphipathic α-helix, which binds via the hydrophobic side chains of the Val74, Leu78, Ile81 and Ile85 residues into a hydrophobic groove on the surface of Bcl- xL (Figure 2).[27] Investigations with mutant Bak peptides showed that the peptide binds as an amphipathic α-helix. Hydrophobic interactions between the side-chains of Val574, Leu578, Ile581 and Ile585 of Bak and a hydrophobic groove formed by Tyr101, Leu108, Val126 and Phe146 on the surface of Bcl-xL contribute the majority of the interaction affinity. In addition, Asp583 of the Bak peptide and Arg139 of Bcl-xL form an important electrostatic interaction. The identification of key interactions across a short peptide epitope encouraged the development of small molecule inhibitors of the interaction.

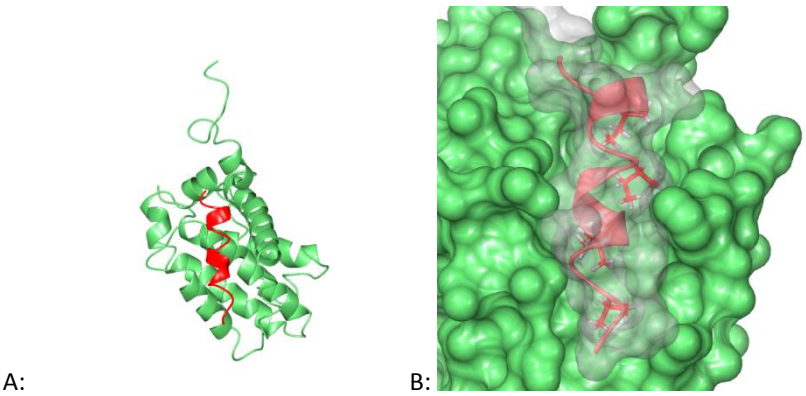

Figure 2: NMR solution structure of Bcl-xL (green) bound to a peptide of residues 572-587 of Bak (red) (pdb 1BXL).[27] A: ribbons; B: Bcl-xL surface (green) and Bak (red with grey surface) showing the key sidechain interactions.

Small molecule Bcl family inhibitors

α-Helix mimics based on a terephthalamide scaffold have been designed to mimic the side chain interactions of the Bak peptide as Bcl-xL inhibitors. Compound **7** inhibits the BH3 domain of Bak binding to Bcl-xL with a similar affinity to the peptide (K_i = 0.78 μM)(Figure 3).[28] Such compounds offer additional validation of the tractability of the Bcl-xL PPI as a target for small molecule inhibitors. However, the poor physicochemical properties of the compound (e.g. cLogP 7.4) prevent their optimisation as drugs.

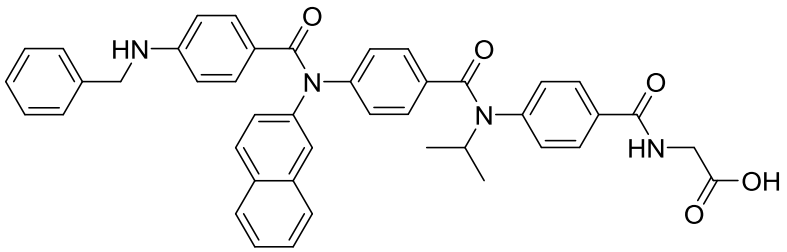

7

Figure 3: Terephthalamide α-helix mimic (**7**).

Screening of a library of natural products using NMR and fluorescence polarisation (FP) assays identified Gossypol (**8**) and Purpurogallin (**9**) as competitive inhibitors of the binding of a labelled BH3 peptide to Bcl-xL (K_i = 0.3 and 2.2 μM, respectively)(Figure 4). Binding to Bcl-xL BH3 binding pocket was confirmed by NMR. Gossypol induces induces multiple cellular effects, some of which can be attributed to it acting as a BH3 mimetic.[29] Despite known liabilities of undesirable redox chemistry and protein reactivity for polyphenolic compounds,[30] Gossypol and (*R*)-gossypol (AT-101) have been evaluated in clinical trials, but with limited efficacy observed in breast and prostate cancer.[31–33]

A structure based approach was used to design a series of Bcl-2 inhibitors based on the docked structure of Gossypol (**8**) bound to Bcl-2.[34] The most potent compound TW-37 (**10**) retains the extensive hydrogen-bonding of one triphenolic moeity combined with a larger hydrophobic group. The second half of **8** is replaced with a hydrophobic amide that allows more extensive contacts with the BH3 binding pocket resulting in improved potency. **10** inhibits Bcl-2, Bcl-xL, and induced myeloid leukemia cell differentiation protein (Mcl-1) interactions (K_i = 0.29, 1.1. and 0.26 μM, respectively) and induces apoptosis in the PC3 prostate cancer cell line (GI_{50} = 200 nM).

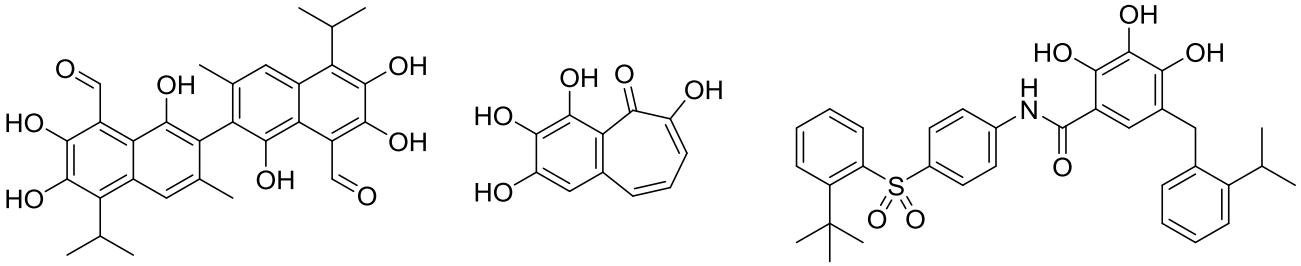

8 **9** **10**

Figure 4: Bcl-2 inhibitors Gossypol (**8**),Purpurogallin (**9**), and TW-37 (**10**).

Fragment based screening offers an alternative to the optimisation of relatively high molecular weight hits from screening library compounds or natural products. Bcl-2 family inhibitors have been discovered and optimised using "SAR by NMR". This is a two step method, in which the first step identifies low molecular weight fragments by observing chemical shift changes in the ^{15}N- or ^{1}H-HSQC NMR spectrum of the protein on binding of the ligand. In the second step, additional fragments occupying different binding sites close to the first fragment hits are identified. NMR or X-ray crystallography are used to determine binding site and orientation of both fragments prior to the design of a suitable linking group. The linked fragments should result in a higher affinity ligand that accesses both binding sites.[35]

Fragments binding to two subpockets of the BH3 interacting-domain death agonist (Bid) BH3 domain were identified in an NMR screen.[36] The interaction sites of the fragments were mapped to specific amino acids on the Bid surface using additional NMR experiments and docking used to determine the likely binding modes. A small library of sulfonamides was prepared to evaluate linking of the fragments together, giving rise to sulfonamide **11** (Figure 5). Binding of **11** to the Bid BH3 domain was confirmed by NMR. Compound **11** was able to inhibit t-Bid induced Smac release in a mitochondrial assay and t-Bid induced apoptosis in transformed HeLa cells. Although further developments to this series have not been reported, this study confirmed the tractability of BH3 domains for NMR based fragment screening and the utility of the fragment linking approach.

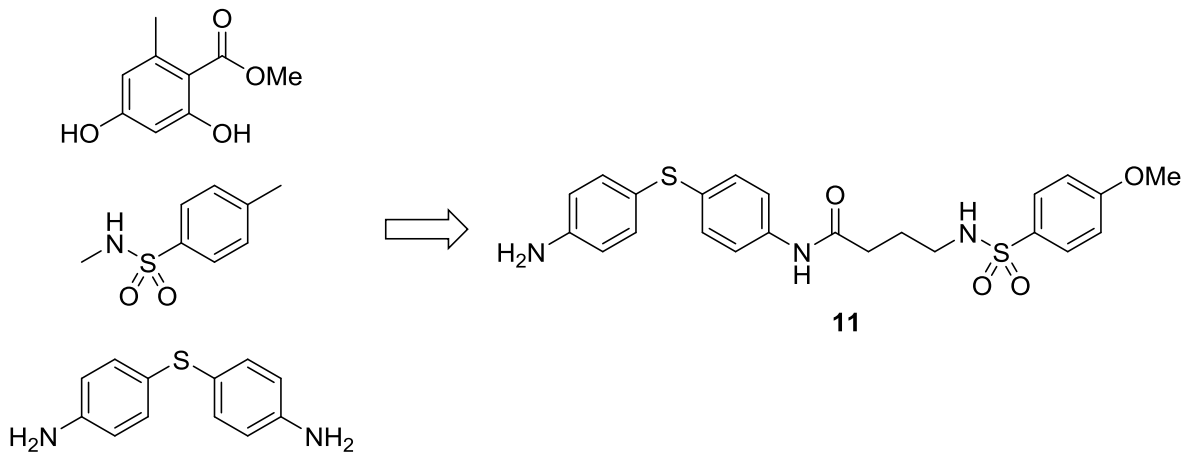

Figure 5. Linking of Bid BH3 fragment hits.

Another application of the SAR by NMR method gave rise to fragment hits for Bcl-xL that bound with millimolar potency. Modification of the fragment bound to Site 1 to an acylsulfonamide allowed linking to the second fragment site and maintained the acidic hydrogen (Figure 6). Parallel synthesis identified compound **12** (K_i = 36 nM), incorporating the 3-nitro-4-(2-phenylthioethyl)amino phenol group that both acts as a linker and occupies the second fragment site. Structure-guided optimisation of **12** allowed the identification of modifications to reduce binding to human serum albumin (HSA) whilst maintaining affinity for Bcl-xL. The replacement of one phenyl ring with a piperazine ring reduced binding to HSA and allowed the introduction of a biphenyl group, as seen in compound **13**, binding deep into a hydrophobic cleft on Bcl-xL that is not seen in the peptide bound structure. The addition of a basic group to the thioethylaminoethyl group further reduced HSA binding giving ABT-737 (**13**).[37,38]

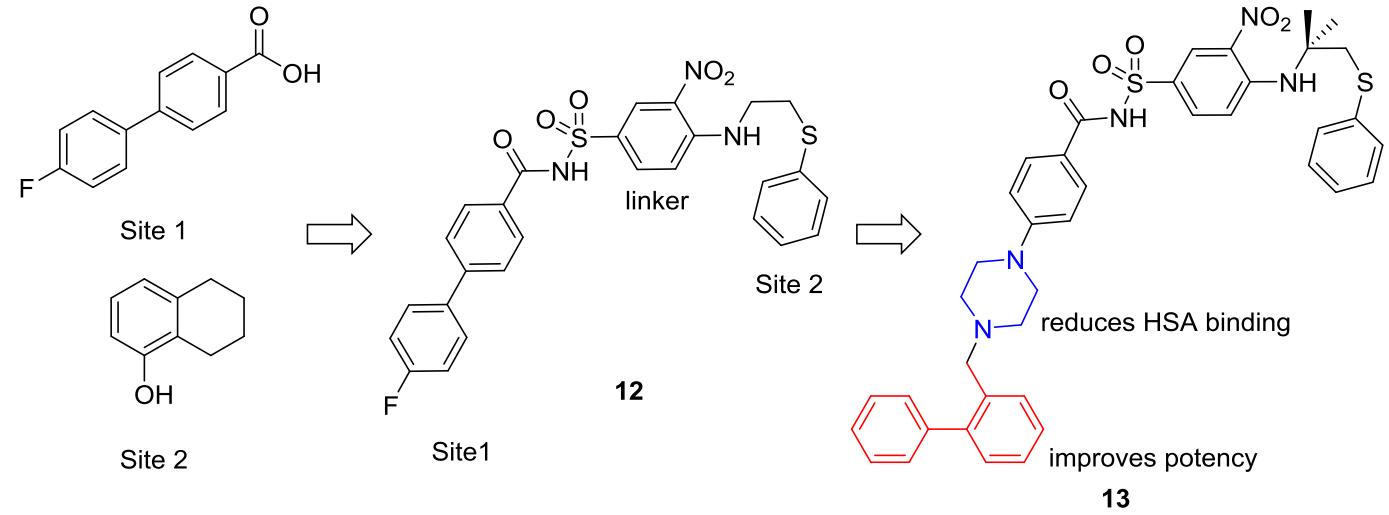

A:

B: 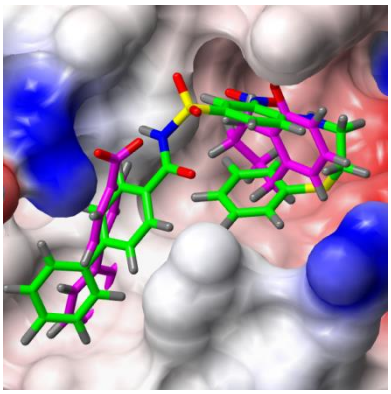

C: 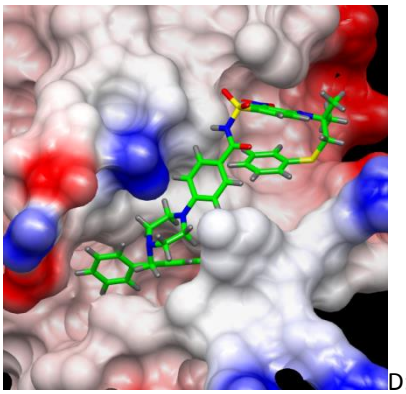

D: 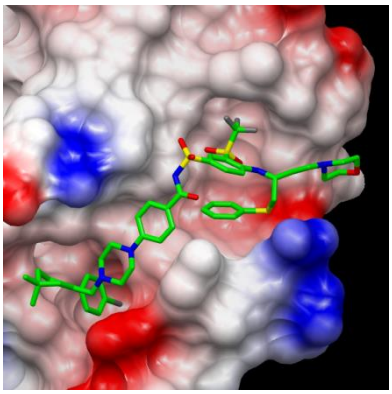

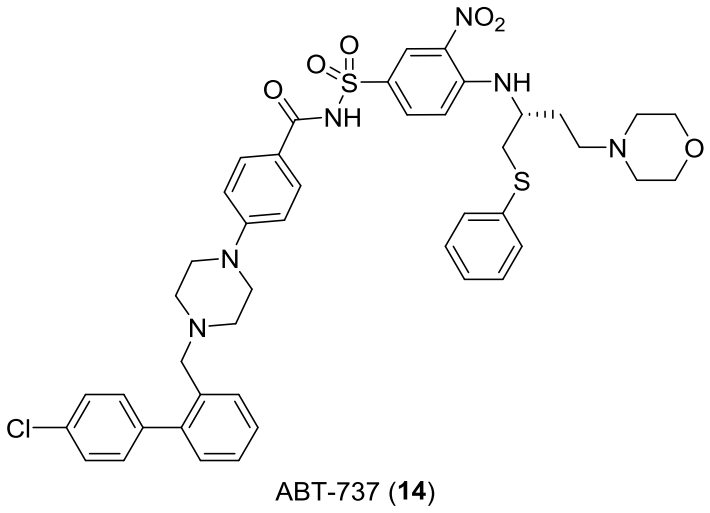

E: ABT-737 (**14**)

Figure 6: A: Linking of Bcl-xL bound fragments and optimisation by linking and structure-based design; B: solvent accessible surface of the NMR structure of Bcl-xL with **12** (green) bound (1YSI), overlayed with fragments (magenta) from 1YSG; C: solvent accessible surface of the NMR structure of Bcl-xL with **13** (green) bound (2O2N); D: solvent accessible surface of the X-ray structure of Bcl-xL with **14** (green) bound (4LVT); E: chemical structure of ABT-737 (**10**).

ABT-737 (**14**) binds potently ($K_i \leq 1$ nM) to Bcl-xL, Bcl-2, and Bcl-2-like protein 2 (Bcl-w) proteins, but less well to family members with lower homology, e.g. B-cell lymphoma/leukemia 11B protein (Bcl-B), Mcl-1 and Bcl-2-related protein A1 (K_i = 460 nM and > 1000 nM, respectively). In cells, **14** acts in a similar manner to an apoptosis sensitising Bad-BH3 peptide by binding to and inhibiting anti-apoptotic Bcl-2 proteins thus removing their protection from apoptosis. **14** does not directly cause cytochrome c release or directly activate the pro-apoptotic proteins Bak and Bax. **14** showed synergism in combination with chemotherapeutics (2-20 fold) and radiation (2-4 fold). **14** induced tumour regression in Bcl-2 overexpressing small cell lung cancer (SCLC) xenografts (100 mg/kg/day ip) and showed improved activity in combination with etoposide.[39]

Promising results with ABT-737 prompted further rounds of structure-guided optimisation resulting in Navitoclax (ABT-263, **15**).[40] In this case modifications were designed that did not disrupt the core binding motif and aimed to optimise aqueous solubility, cellular activity, and ultimately oral bioavailability. Modulation of the acidity of the sulfonamide group by variation of the 3-nitro group enhanced oral bioavailability, and switching the basic dimethylamino group to a morpholine reduced metabolism and improved oral exposure. A 3-trifluoromethylsulfone group proved to be the optimal replacement for the nitro group. Modifications to the 4-chlorobiphenyl moiety gave improved metabolic stability and cellular activity when the internal phenyl ring was replaced with a cyclohexenyl or *gem*-dimethylcyclohexenyl group. ABT-263 (**15**) has a high molecular weight (974 Da) and falls outside of other commonly used drug-like parameters, indicating the difficulty of addressing relatively long lipophilic binding sites. However, **15** shows cellular activity including mechanism-based cytotoxicity in Bcl-2 or Bcl-xL dependent models, and has acceptable oral bioavailability and PK properties.[41] *In vivo* efficacy with complete regressions was observed in SCLC and acute lymphoblastic leukaemia (ALL) based xenografts (100 mg/kg qd p.o.). Reversible thrombocytopenia was noted as a mechanism related toxicity.

A selective Bcl-2 inhibitor was designed with the aim of avoiding the thrombocytopenia observed with **15**, attributed to the inhibition of Bcl-xL, and so improving the theraputic window.[42] In order to separate Bcl-2 binding from Bcl-xL , a series of compounds was prepared starting from **15** with the removal or replacement of key binding moieties. Removal of the thiophenyl group of **15** (e.g. **16**) allowed the key hydrophobic interaction to be achieved from a different vector with an azaindole group, and optimisation of the *gem*-dimethylcyclohexenyl group resulted in the discovery of venatoclax (ABT-191, **17**)(Figure 7). Venatoclax (**17**) is a potent Bcl-2 inhibitor (K_i < 0.01 nM) with good selectivity over Bcl-xL and Bcl-w (K_i = 48 and 245 nM, respectively). Selective cellular activity was seen for **17** in Bcl-2 dependent lines but not in Bcl-xL lines. *In vivo* antitumour activity was demonstrated for **17** in a selection of haematological tumour xenografts on a single oral dose. *Ex vivo* studies with human platelets showed that **17** was significantly less toxic than **15**.

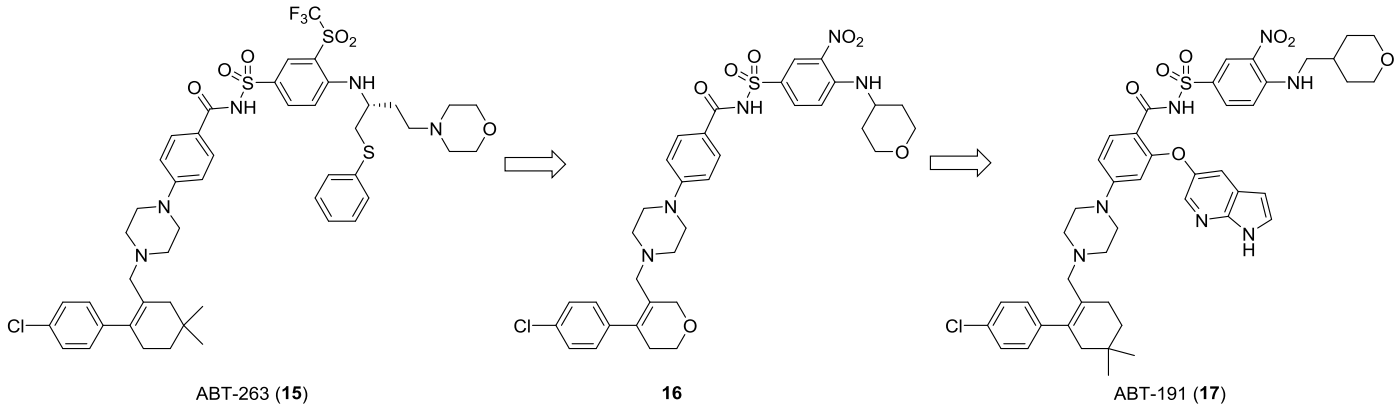

Figure 7: Design evolution of ABT-191 (**17**) from ABT-263 (**15**).

Obatoclax (**18**) was identified in an FP assay measuring the displacement of a BH3 peptide from Bcl-2 family proteins as an inhibitor Bcl-2, Bcl-xL, Mcl-1, Bcl-w, A1, and Bcl-B (Ki ≈ 1-7 µM).[43] Docking to the Bcl-2 NMR structure predicted that **18** binds to the BH3 binding groove in a hydrophobic pocket. The hydrophobicity of **18** (cLogP > 4) was expected to favour membrane localisation, so studies with isolated mitochondria were used to demonstrate disruption of Mcl-1-Bak interactions. In whole cells, treatment with **18** initiates apoptosis, and is able to overcome Mcl-1 overexpression induced resistance to the Bcl-2 inhibitor ABT-737 (**14**) and bortezomib. Single agent antitumour activity was demonstrated in SCID mice bearing human C33A cervical carcinoma tumors with IV dosing at 0.25 and 0.5 mg/kg. A Phase I dose finding study with obatoclax in various tumour types by IV infusion established the tolerability and pharmacokinetics of the drug with some indication of clinical activity.[44]

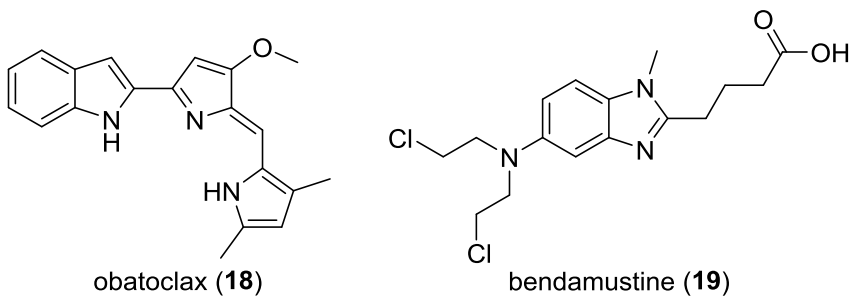

Figure 8: Obatoclax (**18**) and bendamustine (**19**)

Clinical development of Bcl-2 inhibitors

Three Bcl-2 family inhibitors have progressed to clinical trials. Given the central role Bcl-2 family proteins play in the development of many lymphomas, this has been a key focus of clinical studies. A Phase I study with the pan Bcl-family inhibitor Navitoclax (**15**) in relapsed or refractory lymphoid malignancies established the optimum dosing regimen, pharmacokinetics, pharmacodynamics and tolerability of the drug and demonstrated some efficacy.[45] Chronic lymphocytic leukemia (CLL) is characterised by over-expression of Bcl-2, and a Phase I study in CLL with **15** demonstrated substantial efficacy.[46] In SCLC and other solid tumours, a Phase I clinical trial with **15**, under intermittent or continuous oral dosing schedules, established a maximum tolerated dose and demonstrated the safety of the drug and antitumour activity was observed.[47] A Phase IIa single-agent trial of **15** in SCLC also demonstrated safety and biomarker modulation, however, efficacy was limited.[48] Clinical studies with **15** in solid tumours are ongoing as a single agent and in combination with other therapies.

Despite promising results with **15**, the Bcl-xL induced thrombocytopenia observed was dose limiting and so attention switched to the Bcl-2 selective inhibitor venatoclax (**17**).[49] A single agent Phase I study of **17** in CLL and small lymphocytic leukemia (SLL) showed an 84% response rate in CLL patients without significant reports of thrombocytopenia.[50] A Phase II study of **17** in ALL demonstrated activity in this indication, particularly in patents with a poor prognosis.[51] A combination of **17** with the anti-CD20 antibody rituximab was evaluated to determine the maximum tolerated dose and safety profile, producing an overall response rate of 88% with good tolerability.[52] A phase 1b combination study of **17** with bendamustine (**19**) in relapsed non-Hodgkin lymphoma established the safety of the combination, and showed good evidence of efficacy.[53] A Phase 2 study of **17** in relapsed

or refractory CLL patients with a chromosome 17p deletion showed an 80% response rate, demonstrating the effectiveness single agent **17** in a patient group that responds poorly to immunotherapy.[54] On the basis of these results venatoclax (**17**) received accelerated clinical approval in the US and Europe.

In a phase I trial with obatoclax (**18**) in advanced CLL acceptable safety, and phamacodynamic responses (Bax and Bak elevation) were observed. Modest single agent activity was seen with 1/26 patients achieving a partial response.[55]

MDM2-p53

Biology

The p53 tumour suppressor acts as a central node in the cellular response to stress and DNA-damage.[56] Activation of p53 produces an active tetramer that can transcribe around 150 genes, giving rise to a number of cellular effects including initiating apoptosis, cell-cycle arrest, DNA-repair, senescence or altered metabolism.[57] MDM2, itself a product of p53 mediated transcription, acts as a negative repressor of p53 by binding to and occluding the p53 transactivation domain and by acting as an E3-ubiquitin ligase, targeting the complex for proteasomal degradation.[58,59] The MDM2-p53 interaction forms an autoregulatory feedback loop, ensuring that cellular activation of p53 is transient.

Amplification of the *MDM2* gene and overexpression of MDM2 protein occurs in around 10% of common cancers. The highest incidence is found in hepatocellular carcinoma (44%), lung (15%), sarcomas and osteosarcomas (28%), and Hodgkin disease (67%).[60] MDM2 overexpression overrides p53 activation and inactivates its tumour suppressor function, thus rendering the cells effectively p53 null.

Inhibitors of the MDM2-p53 PPI have been sought as they should act to reactivate p53-mediated cell death by removing MDM2 mediated repression of transcription. Tumour selectivity is predicted to result from the removal of a MDM2 block on pre-existing DNA-damage or oncogenic activation signals, thus allowing p53-mediated activation of apoptosis.

Structural biology and peptides

The NMR structure of MDM2 reveals that the protein adopts multiple conformations,[61] with residues 16-24 of the N-terminal region forming a flexible lid that closes over the p53 binding site.[62] p53 easily displaces the lid to form a more stable complex.[63] The X-ray structure of a p53 peptide and MDM2 interaction shows the surface MDM2 forms a hydrophobic cleft into which the p53 peptide binds as an amphipathic α-helix (Figure 5A).[64] Epitope scanning determined that three p53 residues, Phe19, Trp23, and Leu26, form the principle interactions with MDM2, secured by two intermolecular hydrogen-bonds, between the backbone of Phe19 of p53 and the Gln72 side chain of MDM2, and between the p53 Trp23 indole NH and the backbone carbonyl of Leu54 from MDM2 (Figure 9A). Potent inhibitors of the MDM2-p53 interaction were discovered from synthetic peptide libraries, including the AP peptide (IC_{50} = 5 nM) that incorporates 6-chlorotryptophan, and phosphonomethylphenylalanine residues.[65] The X-ray structure of the AP peptide bound to MDM2 (Figure 9B) shows the 6-chlorotryptophan group occupies additional space below the Trp23 site, and makes additional van der Waals contacts with Phe86 and Ile99 of MDM2.

Hydrocarbon stapled α-helical peptides e.g. SAH-p53-8, Ac-QSQQTF*NLWRLL*QN-NH_2 (* indicates the position of the hydrocarbon staple), have shown excellent potency as MDM2-p53 inhibitors.[66,67] The X-ray crystal structure of SAH-p53-8 bound to MDM2 shows that the key binding residues Phe19, Trp23, and Leu26 form part of a short α-helix that binds to MDM2 (Figure 9C).[68] SAH-p53-8 induces p53 mediated cytotoxicity in MDM2 overexpressing cells. Similarly, the stapled peptide ATSP-7041, Ac-LTP*EYWAQAba*SAA-NH_2, is a potent dual inhibitor of both MDM2-p53 (K_i = 0.9 nM) and MDMX-p53 (K_i = 6.8 nM), which has been optimised for solubility, and cellular potency.[69] The X-ray structure of ATSP-7041 bound to MDMX shows that the hydrocarbon staple makes significant interactions with the protein and so contributes to binding affinity. ATSP-7041 showed activity *in vivo* in MDM2 and MDMX overexpressing human tumour xenografts. Other peptide derived MDM2-p53 inhibitors using alternative backbones have been invesigated with varying success including reteroinverso D-peptides,[70,71] β-peptides,[72–74] di-proline β-hairpins,[75,76] and peptoids.[77]

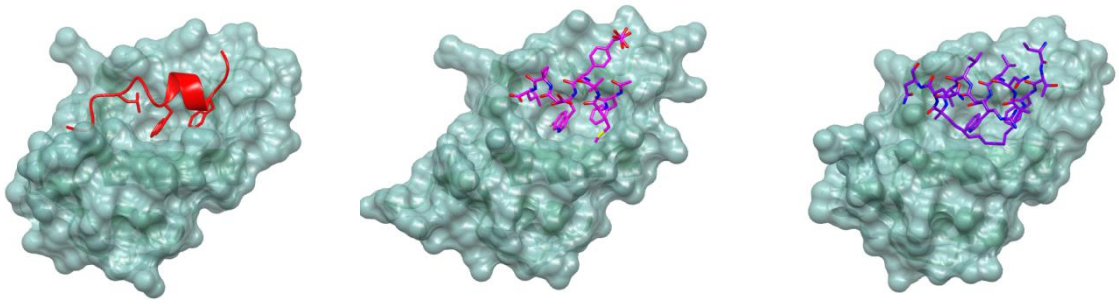

A: B: C:

Figure 9: X-ray structure of MDM2 (ribbon – green, surface – light green) bound to A) residues 15-29 of p53 showing the key hydrophobic sidechains (red) (pdb 1YCR), B) AP peptide (magenta)(pdb: 2GV2) C) SAH-p53-8 (purple)(pdb: 3V3B)

Hit discovery and optimisation

A variety of peptide mimetic approaches have been employed, using differing structures to array side chains in the appropriate orientation to recapitulate the peptide interaction with the MDM2 binding cleft (Figure 10).[78] Terphenyls e.g. **20** demonstrated the validity of this approach.[79] α-Helix mimics based on an oligoamide scaffold (**21** and **22**) were weak MDM2-p53 inhibitors.[80,81] The α-1,4 linked oligogalactose **23**, bearing groups corresponding to the important p53 side chains from alternate C-6 and C-3 hydroxyl groups, showed weak MDM3-p53 inhibitory activity.[82] Although these approaches offer interesting insights into the binding requirements for MDM2, the compounds' high molecular weights and poor drug-like properties prevent their development.

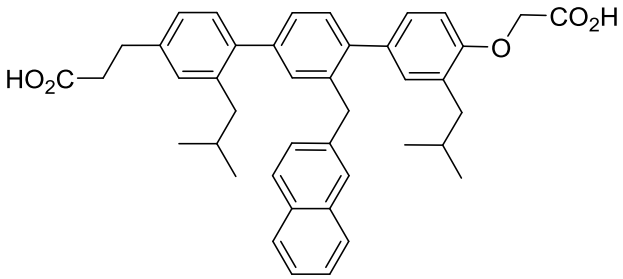

20

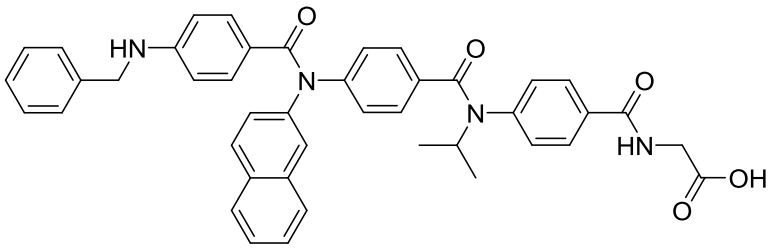

21

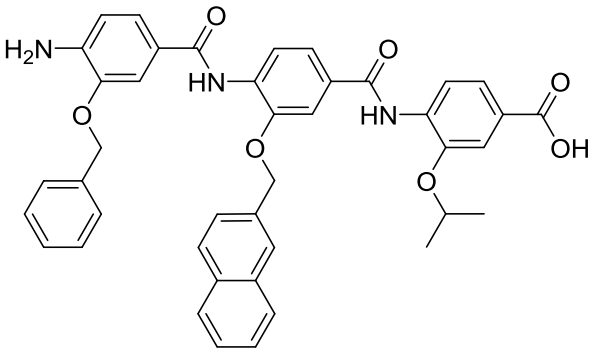

21

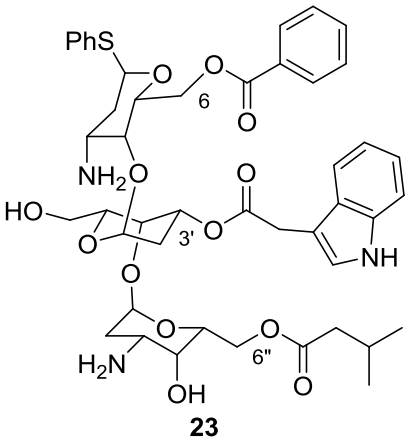

23

Figure 10: α-helix mimetic MDM2-p53 inhibitors

The Nutlins are *cis*-imidazoline containing compounds, which were identified by HTS as inhibitors of MDM2-p53 with IC_{50} values in the 100-300 nM range (e.g. **24,** IC_{50} = 90 nM).[83] The series yielded the first reported X-ray and NMR structures of small molecules in complex with MDM2, showing that the heterocyclic scaffold arrays its substituents to mimic the side-chains of an α-helical peptide (Figure 11A, pdb 4J3E).[84] Structure-guided optimisation enabled improvements to stability at the imidazoline heterocycle by the introduction of two *cis*-methyl groups and modification the metabolically labile 4-methoxy group to a *tert*-butyl group. Additional potency and favourable PK properties were gained by the addition of a hydrophilic sulfone chain to the piperazine moiety, giving rise to the clinical candidate RG-7112 (**25,** IC_{50} = 18 nM). The X-ray co-crystal structure of MDM2 with **25** (Figure 11B) shows it has a similar binding mode to Nutlin-3a, with the methylsulfone side chain extending into solvent.

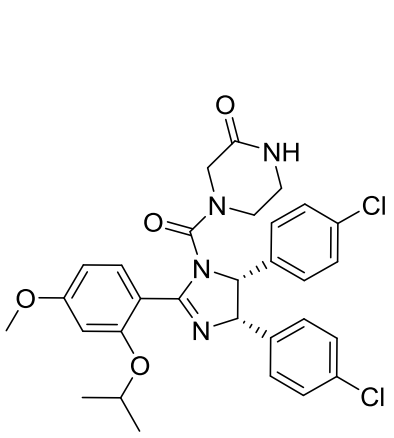

24

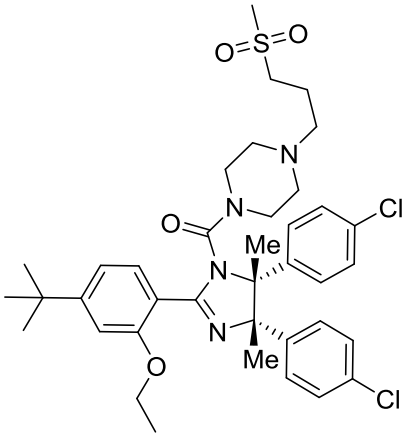

25

A: 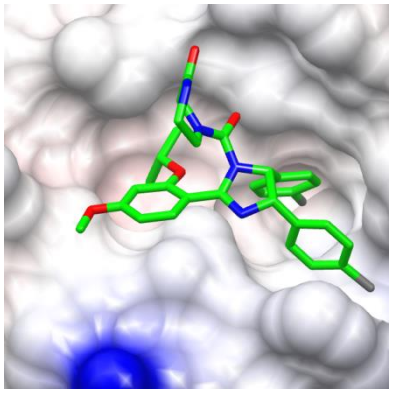 B: 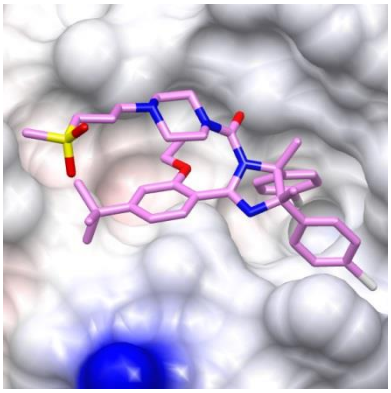

Figure 11: X-ray structure of MDM2 (electrostatic surface) bound to A) Nutlin 3a **24** (green) (pdb 4J3E), B) RG7112 **25** (pink)(pdb: 4IPF)

Modification of the Nutlin scaffold to a dihydroimidazothiazole resulted in the identification of a series of potent MDM2 inhibitors, such as **26** (IC_{50} = 90 nM). Addition of the 6-methyl group is sufficient to stabilise the imidazoline ring to oxidation.

The bicyclic scaffold orientates the 3-isopropyl group into the MDM2 Phe19 pocket, and addition of an amide at the 4-position gave additional potency.[85,86] The X-ray structure of **26** bound to MDM2 shows the imidazole ring and chlorophenyl groups occupying similar space to the Nutlin series (Figure 12A). The thiazole and isopropyl groups fill space occupied by the alkoxyphenyl group of **24**, and the amide side-chain occupies a surface groove formed by the movement of a flexible loop. Interactions in the Trp23 binding pocket were optimised by the addition of a 3-fluoro-4-chlorophenyl group, and the amide moiety was elaboration with a 4,7-diazaspiro[2,5]octane group giving DS-5272 (**27**, IC_{50} = 24 nM, Figure 12B).[87] DS-5272 showed good cellular activity, solubility, microsomal stability and acceptable *in vivo* PK properties. Anti-tumour efficacy was demonstrated in a MDM2-amplified mouse xenograft model (50 mg/kg/qdx4 p.o.). The authors suggest that DS-5272 is a possible candidate for clinical development, but the structure of the clinical candidate DS-3032b has not been disclosed.

A: 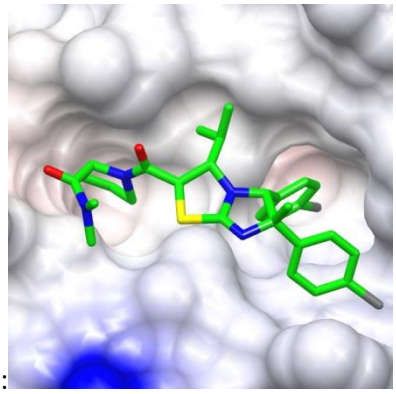 B: 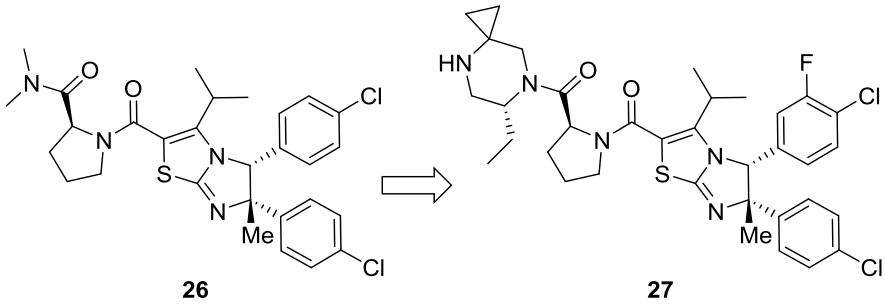

Figure 12: A) X-ray structure of MDM2 (electrostatic surface) bound to dihydroimidazothiazole **26** (green) (pdb 3VZV), B) Design evolution of DS-5272 (**27**) from **26**.

A series of spirooxindoles, e.g. **28** (K_i = 86 nM), were identified initially by substructure searching for oxindole containing natural products designed to mimic the tryptophan of p53 (Figure 7).[88] Structure-based elaboration of the amide group and addition of a 5-fluoro group resulted in improved potency, e.g. **29** (IC_{50} = 28 nM).[89,90] The X-ray co-crystal structure of **29** bound to MDM2 shows the oxindole ring occupying the Trp pocket, with hydrogen bonds between the oxindole NH and the backbone carbonyl of Val54, and His96 NH and the amide side-chain carbonyl group, the 3-chloro-2-fluorophenyl group fills the Leu pocket, and the *t*-butyl group is in the Phe pocket (Figure 8). The diol MI-147 (**31**, IC_{50} = 16 nM) showed cellular activation of p53 and *in vivo* activity in an MDM2 amplified tumour xenograft. Importantly, spirooxindoles e.g. **30** were found to epimerise under oxidative conditions to diastereomeric mixtures and the most stable diastereoisomer proved to have improved potency and *in vivo* activity.[91,92]

SAR405838 (**32**, *Ki* = 0.88 nM) was selected from a series of amides as it showed improved chemical and metabolic stability, in addition to potent MDM2 binding affinity, selectivity, and growth inhibitory activity.[93] Spiroxindole **32** induced complete tumour regression in SJSA-1 mouse xenografts with a single oral dose (100 mg/kg) and on repeat dosing. The *in vivo* efficacy of **32** was also demonstrated in a multiple tumour types without *MDM2* amplification. Consequently, **32** was selected as a clinical candidate from the spirooxindole series.

Further structure-guided optimisation of the spirooxindole series aimed to remove instability due to epimerisation.[94] Replacement of the 2'-neopentyl group of **32** with a cyclohexyl ring removed one chiral centre and maintained interactions in the Phe19 pocket of MDM2. Introduction of a carboxylic acid to the amide side-chain improved cell-free potency with the bicyclo[2.2.2]octane moiety as a phenyl ring replacement conferring improved PK characteristics. The alkylation of the pyrollidine nitrogen was necessary to improve the cellular PD response of the compound. The resulting compound APG115 (**33**) showed anti-tumour efficacy in a SJSA-1 mouse xenograft model (100 mg/kg/qd p.o.) and has entered phase I clinical trials.

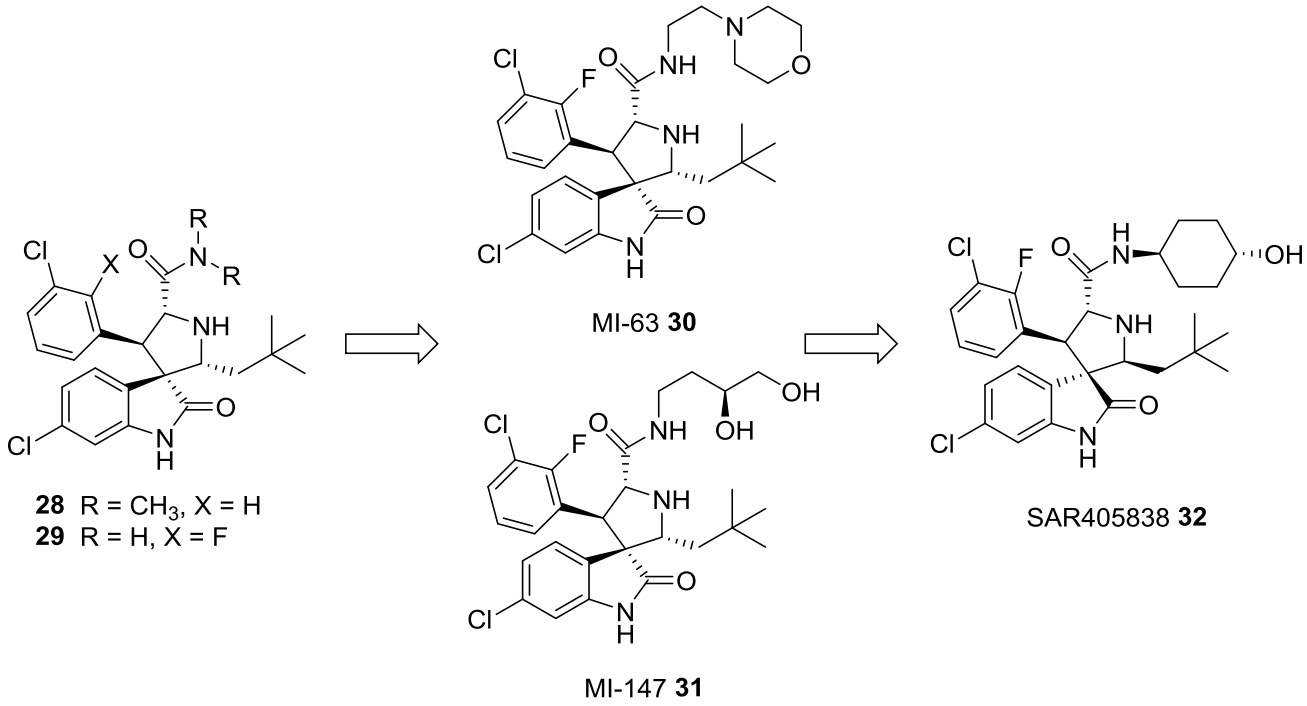

Figure 13: Design evolution of SAR405838 (**32**) from **28**.

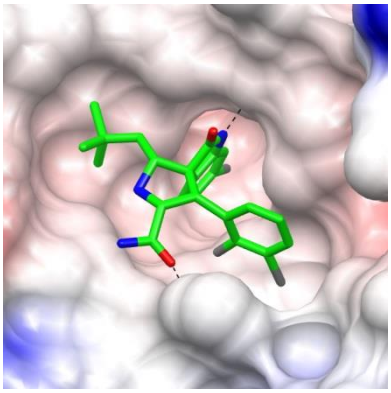

Figure 14: X-ray structure of MDM2 (electrostatic surface) bound to oxindole **29** (green) (pdb 3LBL).

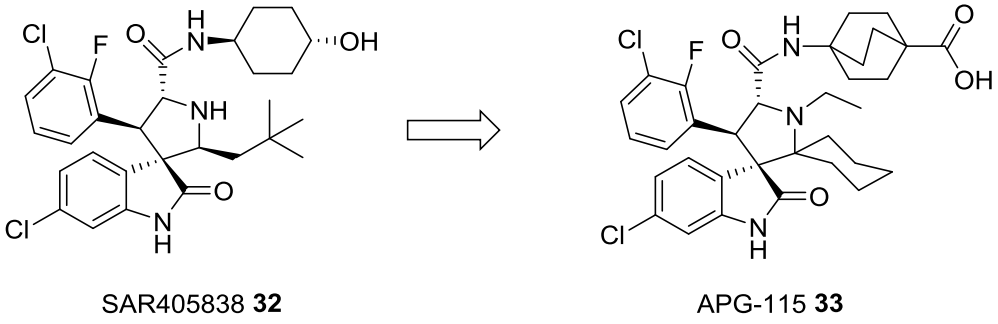

Figure 15: Design of APG115 (**33**) from **32**.

The spirocyclic amide scaffold of spirooxindole **32** was simplified to a cyanopyrrolidine core allowing a "*cis*" configuration of aromatic groups e.g. **34** (IC_{50} = 196 nM).[95] The X-ray co-crystal structure of **34** bound to MDM2 shows the 4-chlorophenyl ring occupying the Trp pocket, with a hydrogen bond between His96 NH and the amide side-chain carbonyl group, the 3-chlorophenyl group fills the Leu pocket, with the cyano group projecting into solvent and the *t*-butyl group occupies the Phe pocket (Figure 16). The addition of fluoro substituents to both aromatic rings was found to improve MDM2 inhibitory potency.

Optimisation of the PK profile was achieved at the amide side chain substituent, that was also found to modulate cellular potency. A 4-benzenecarboxylic group gave the desired properties, and SAR studies around the ring revealed that the *ortho*-methoxy group, **35** (RG7388), had the ideal combination of MDM2 binding affinity, cellular potency and selectivity. RG7388 (**35**) gave complete tumour regression *in vivo* in an SJSA-1 xenograft model (25 mg/kg p.o.), and a favourable PK profile. RG7388 (**35**) was selected as the second generation MDM2-p53 clinical trial candidate owing to its improved potency, cellular selectivity and PK properties over RG7112 (**25**).

A: 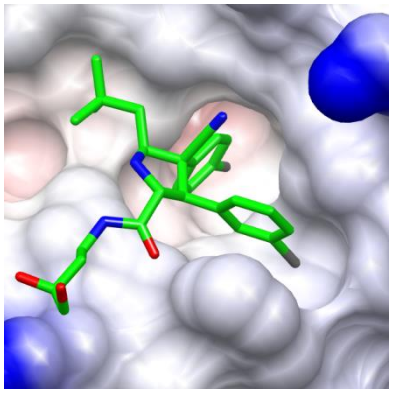 B:

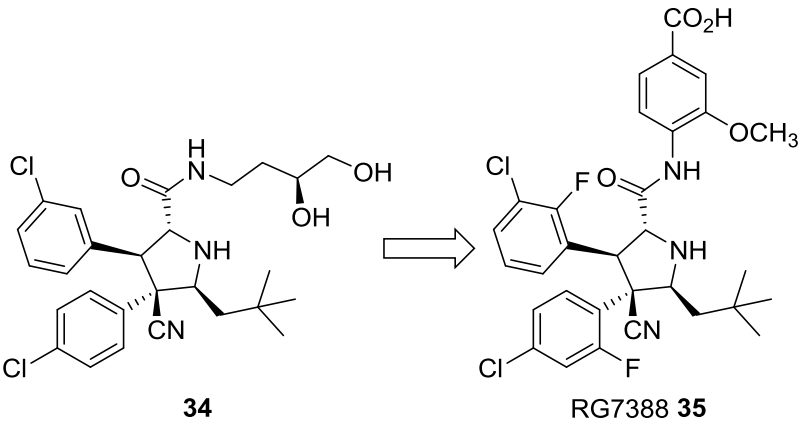

Figure 16: A) X-ray structure of MDM2 (electrostatic surface) bound to cyanopyrrole **34** (green) (pdb 4JRG); B) Design evolution of RG7388 (**35**) from **34**.

Substituted piperidines, e.g. **36** (IC_{50} = 600 nM), were identified as hits from a FP-based HTS (Figure 17A).[96] Introduction of a 2-methoxyethoxyphenyl substituent gave improved potency and the alkyl substituent on the piperidine ring was found to be essential to promote the optimum conformation of the ring e.g. **37** (IC_{50} = 40 nM).[97,98] The MDM2 bound X-ray structure of **36** identified the main interactions as the trifluoromethylpyridine occupying the Phe19 pocket, the trifluoromethylphenyl residue projecting into the Trp23 pocket and the Leu26 pocket filled by the alkoxyphenyl group (Figure 17B). Structure-guided optimisation resulted in **38** (Figure 17C).[99] A combination of a 2-trifluoromethylthiophene replacement for the trifluoromethylphenyl residue and a butanoic acid substituent to the alkoxyphenyl group gave a 5-fold improvement in potency and cellular activity (**38**, IC_{50} = 7 nM). Compound **38** showed single agent activity in an A549 tumour xenograft at 200 mg/kg qd and in combination with taxoids.

A:

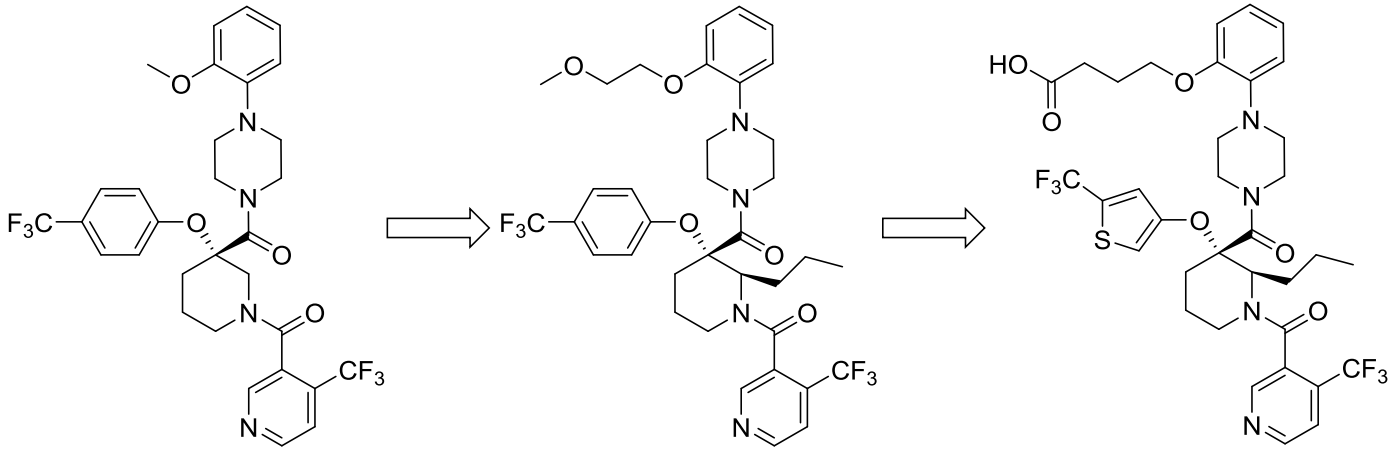

B: 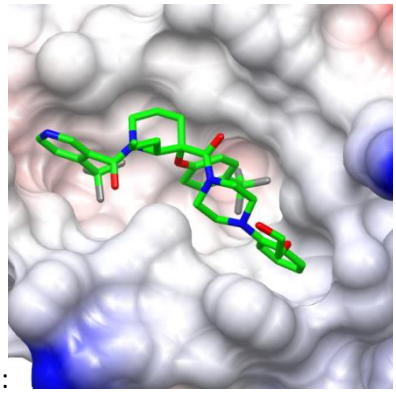 C: 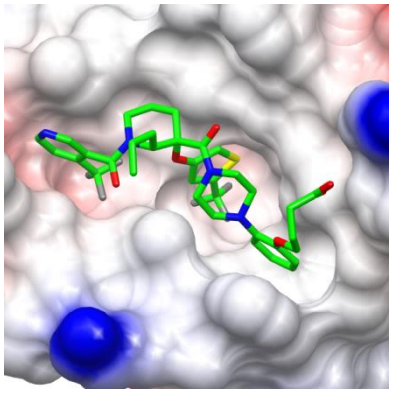

Figure 17: A: Design of piperidine **38;** X-ray structures of MDM2 (electrostatic surface) bound to B: piperidine **37** (green) (pdb 5HMK) C: piperidine **38** (green) (pdb 5HMH).

A structure-based design approach identified the piperidone series of inhibitors (e.g. AM-8553, **39**, IC_{50} = 1.1 nM).[100] An X-ray structure of **39** bound to MDM2 showed that the (3*R*)-carboxyl group at C3 forms a key interaction with His96, the 4-chlorophenyl group occupies the Typ pocket, the 3-chlorophenyl group fills the Leu pocket and the N-alkyl chain projects into the Phe pocket (Figure 18A). Modifications to the *N*-substituent aimed to optimise interactions with the 'glycine shelf' region, a hydrophobic region on the surface of MDM2 formed by Gly58 (Figure 18B).[101,102] Sulfone **40** (AMG 232, IC_{50} = 0.6 nM) showed excellent cell-free potency and cell growth inhibitory activity. Complete tumour regression in SJSA-1 xenografts observed (60 mg/kg/qd p.o.), and so AMG 232 was selected for clinical trials.[103] Additional SAR studies around the carboxylic acid moiety resulted in compounds with equivalent potency.[104,105]

A: 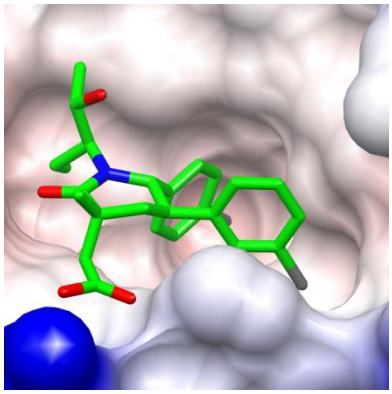 B: 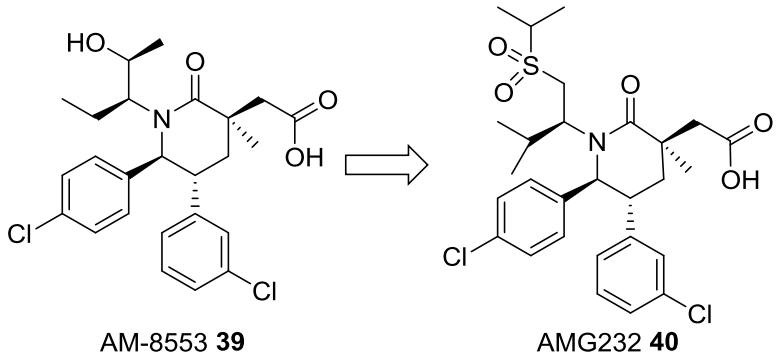

Figure 18: X-ray structure of MDM2 (electrostatic surface) bound to A: AM-8553 **39** (green) (pdb 4ERF) B: Design of AMG232 **40**.

Rational design based on the X-ray structure of the AP peptide bound to MDM2 (Figure 5B) gave rise to the 'central valine' concept, resulting in the identification of substituted imidazole (**41**, IC_{50} = 30 nM)(Figure 19).[106] Structure-guided modifications to optimise potency and solubility gave rise to compound **42** (IC_{50} = 2 nM), however, the cellular activity in this series is poor compared with other series displaying similar MDM2-p53 potency.[107]

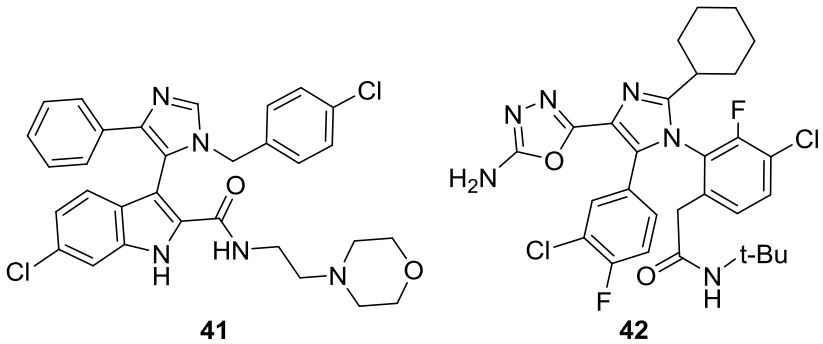

Figure 19: substituted imidazole MDM2-p53 inhibitors (**41** and **42**)

Virtual screening identified dihydroisoquinolinone **43** as a hit MDM2-p53 inhibitor (IC_{50} = 540 nM)(Figure 20A).[108] An X-ray structure of **44** bound to MDM2 showed an unexpected binding mode, significantly different to most MDM2 inhibitors, whereby the Leu26 sub-pocket is occupied by the C7 ethyl ether and not a substituted phenyl ring as seen in the majority of other inhibitor series (Figure 20B). X-ray structure guided optimisation gave rise to **45** (IC_{50} = 8 nM) with excellent cellular activity (Figure 20C). An X-ray structure of **45** showed that chlorophenyl group requires to be in the (*S*)-configuration at C1 and showed opportunities for optimisation around in the Phe pocket occupied by the 4-pyridinyl group (Figure 20C). Replacement of the pyridyl group with a *trans*-cyclohexyl amine gave NVP-CGM097 (**46,** IC_{50} = 1.7 nM) with good cellular and ADME properties.[109] The X-ray structure of **46** bound to MDM2 shows the Trp23 pocket is filled by the C1 4-chlorophenyl group, the Leu26 pocket filled by the C7 isopropyl ether, and the Phe19 sub-pocket is occupied and extended by movement of the protein to accommodate the large amine side-chain (Figure 20D). NVP-CGM097 showed good PK properties in a number of mammalian species and induced tumour regression in SJSA-1 xenografts (30 mg/kg/qd p.o.). NVP-CGM097 (**46**) has been selected for clinical trials.

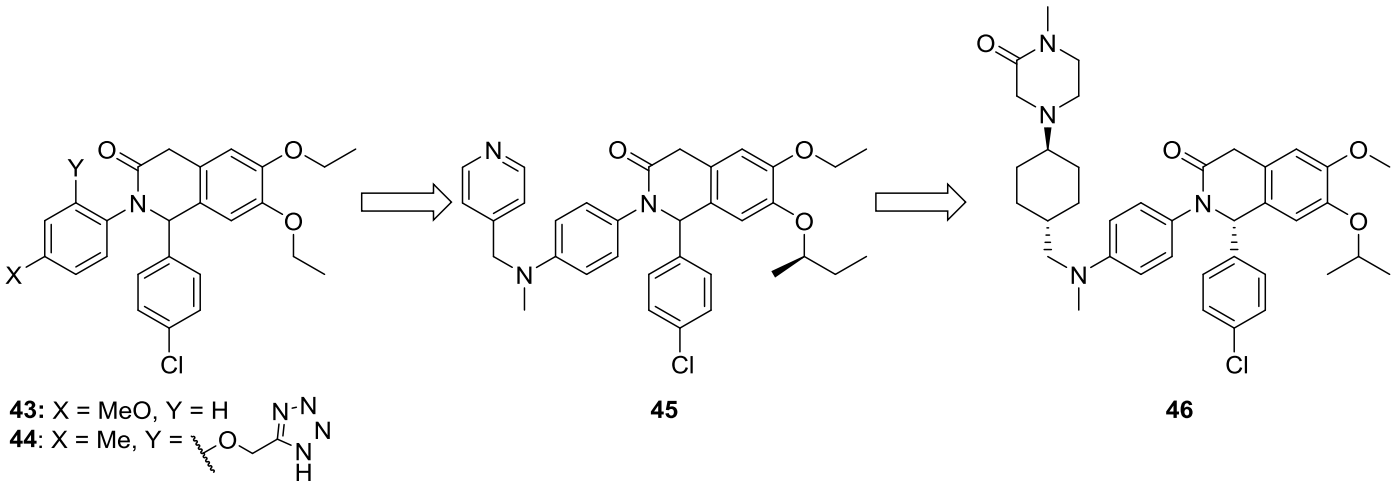

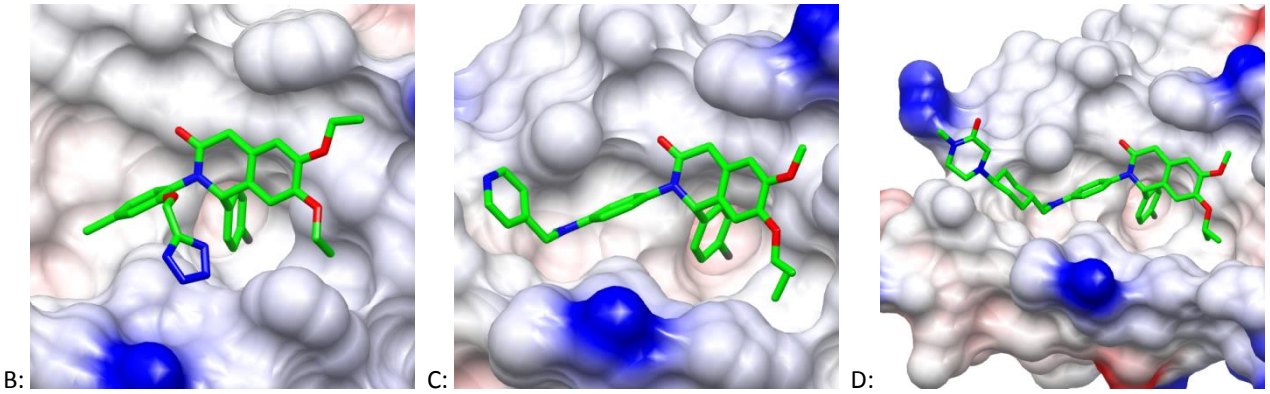

Figure 20: A: Design evolution of NVP-CGM097 (**46**); X-ray structure of MDM2 (electrostatic surface) bound to B: dihydroisoquinolinone **43** (green) (pdb 4ZYC); C: dihydroisoquinolinone **45** (green) (pdb 4ZYI); D: NVP-CGM097 (**46**) (green) (pdb 4ZYF).

In an alternative approach, based on hit compound **41** structural considerations gave rise to a new scaffold comprising a substituted delta-lactam fused to a five membered ring. Substructure searching identified lactam **47** as a novel hit with modest potency (IC_{50} = 1.5 µM)(Figure 21).[110] Elaboration of hit **47** identified structural requirements for potency including, introduction of a 5-chloropyridin-2-one moiety to occuy the Leu23 pocket and stack efficiently with His96. The clinical trial candidate from this series HDM-201 (**48**) was reported recently as a potent inhibitor with favourable PK and PD profiles in animal studies.[111]

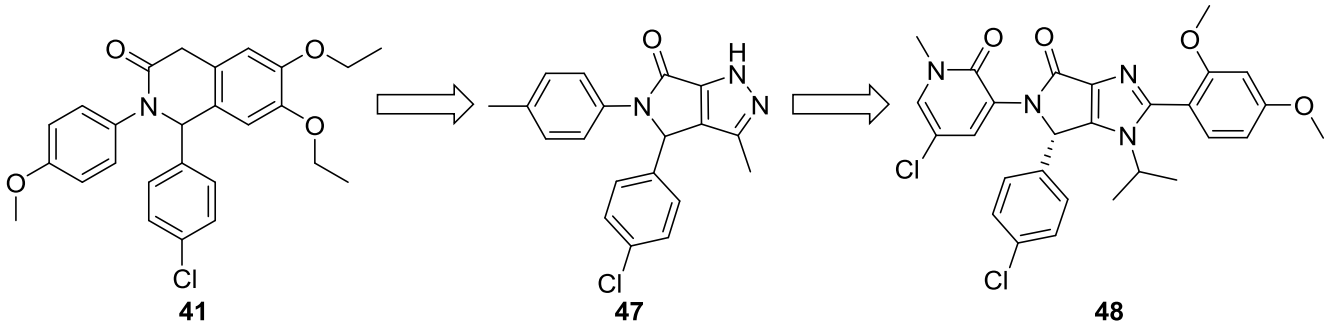

Figure 21: design of HDM-201 (**48**).

Clinical development summary

A number of MDM2-p53 inhibitors have entered clinical trials in solid and haematological malignancies (Table 2). A phase I clinical trial of of RG7112 **25** in liposarcoma patients showed responses to therapy in 16 from 20 patients as partial response or stable disease.[112] A poor PK profile was observed, PD markers for apoptosis and p53 activation showed a linear relationship with drug exposure and a food effect was noted.[113] Some toxicity was observed including neutropenia and thrombocytopenia. A phase I trial of **25** in various leukemias showed activity in patients AML.[114] The second generation inhibitor RG7388 (**35**) is under clinical investigation in a Phase III trial in AML.[115,116] SAR405838 (**32**) was selected as the clinical candidate from the spirooxindole series and entered Phase I clinical trials as a single agent and in combination with the MEK1/2 inhibitor pimasertib. APG-115 (**33**) has entered Phase I clinical trials in advanced solid tumours and lymphomas as a single agent.

A Phase I/II trial of AMG232 (**40**) is ongoing in metastatic melanoma, in combination with the MEK1/2 inhibitor trametinib and the B-Raf inhibitor dabrafinib. DS-3032b has been evaluated in a Phase I trial with some evidence of efficacy, and on target toxicity.[117] Phase I trials of MK-8242 demonstrated some activity in liposarcoma and in AML.[118,119] Results of trials of CGM097 (**46**) and HDM201 (**48**) have not been reported to date.

Overall, a number of agents have shown efficacy in both MDM2 amplified tumours e.g. liposarcomas and AML. Dose limiting p53 mediated on target toxicity, including thrombocytopenia, has been reported. To date, no MDM2-p53 inhibitor has been approved, and the second generation inhibitor RG7388 has advanced the furthest.

SMAC-XIAP

Biology

The inhibitor of apoptosis (IAP) family of proteins inhibit entry into apoptosis at the point of caspase activation.[120] XIAP binds to the *N*-terminal amino acids of caspases 3,7, and 9 via its BIR domains and directly inhibits their activity. The activating Smac promotes apoptosis by binding to XIAP.[121] The ML-IAP proteins bind to Smac, preventing its association with XIAP and so inhibiting apoptosis (Figure 22). The c-IAPs have a different mechanism, acting as negative regulators of the alternative NF-κB pathway by inhibiting NF-kappa-B-inducing kinase (NIK), and as activators of the classical NF-κB pathway by acting on Receptor-interacting serine/threonine-protein kinase 1 (RIPK1). Amplification or overexpression of XIAP is has been observed in haematological and solid tumours, and is linked to poor prognosis and poor response to therapy. Similarly, amplification or overexpression of c-IAPs has been identified in a large variety of tumour types. The role of XIAP at the convergence of multiple apoptotic signaling pathways has made it an attractive target for therapeutic intervention.

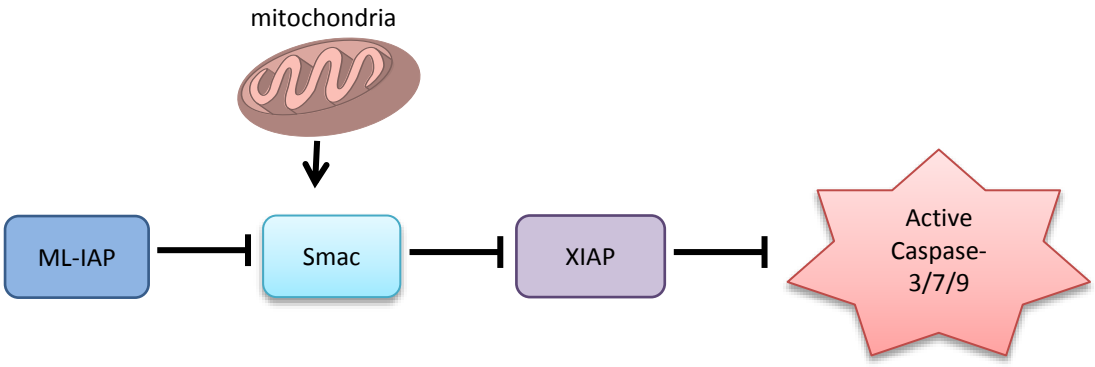

Figure 22: The role of IAP proteins in caspase activation.

Peptides and structural biology

The X-ray structure of Smac bound to XIAP shows the N-terminal four residues of Smac bound to a groove on the surface of XIAP (Figure 23A,B).[122] Validation of targeting the Smac-IAP interaction as a therapeutic strategy was demonstrated using cell-penetrant synthetic peptides including seven N-terminal residues of Smac and a cell penetrating TAT domain were found to sensitise TNF-related apoptosis-inducing ligand (TRAIL)-induced apoptosis and cytotoxic drug treatment in cells, but did not initiate apoptosis as single agents.[123] *N*-Terminal Smac mimetic tetrapeptide libraries established the pharmacophore for the binding to BIR3 (Figure 23C).[124] Modifications of the alanine residue at position 1 are limited to small L-amino acids, e.g. Abu, and retention of the NH is essential. Substitution at position 2 (Val) is tolerated, consistent with this residue projecting into solution, but D-amino acids are not tolerated. The proline ring at position 3 was required for activity, only the 4-membered azetidine substitution was tolerated. Replacement of the isoleucine at position 4, with aromatic rings e.g. Phe or Nal, was favoured. Non-amino acid substituents at position 4 reduced the peptidic nature of the compounds and improved activity e.g. **49** (K_D = 12 nM). Substitution onto the proline ring added potency, e.g. **50** (K_D = 5 nM). Structure based design of peptide inhibitors gave **51**.[125,126]

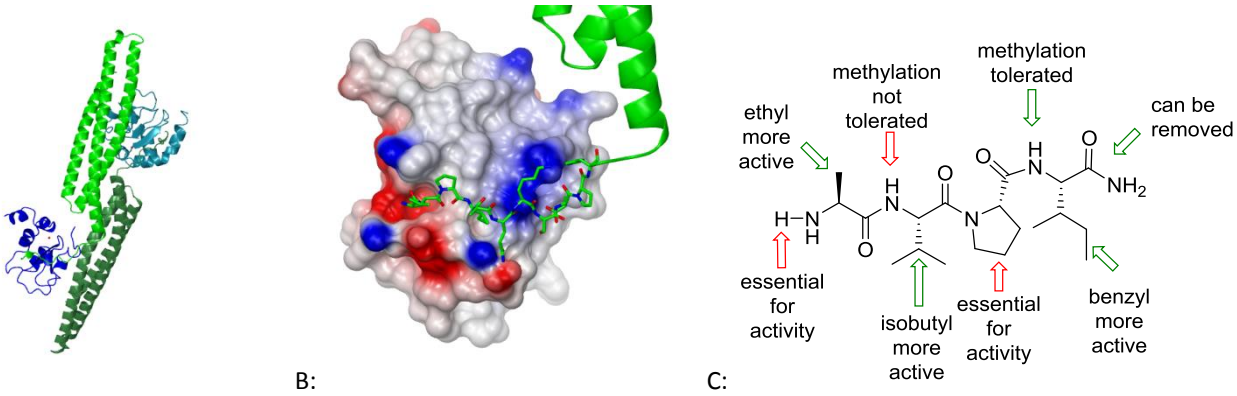

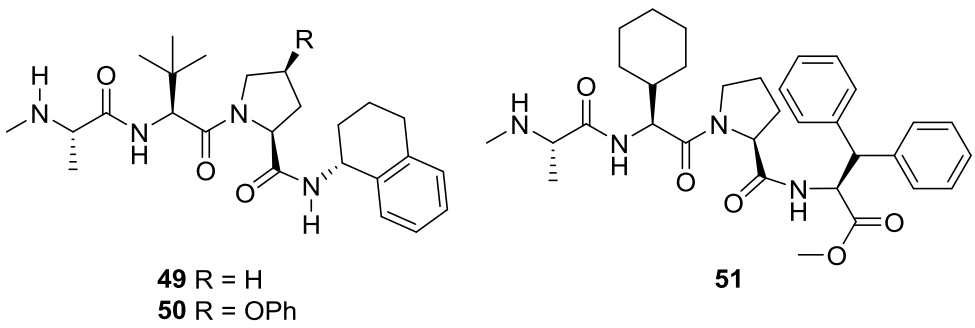

Figure 23: X-ray structure of the BIR3 domain of XIAP complexed to Smac A: dimeric structure of XIAP (Blue) and Smac (Green); B: X-ray structure of the BIR3 domain of XIAP (electrostatic surface) complexed to Smac (green) (pdb 1G73); C: pharmacophore for tetrapeptide Smac-mimetic IAP inhibitors; D: structures of peptide IAP inhibitors **49-51**.

Hit discovery and optimisation

A number of structurally diverse of peptidomimetic scaffolds have been used to develop potent mono-valent Smac mimetics that show a range of selectivity between cIAP-1 and -2 and XIAP. Structure-based design of cIAP selective inhibitors revealed that variations at the P4 amino acid gave good selectivity, 2-pyrimidinyl compound (**52**) was a selective inhibitor of cIAP-1 and -2, but >2000-fold less potent vs XIAP.[127] The selectivity was explained by modelling that showed an adverse lone-pair interaction in the P4 binding pocket between the pyrimidine nitrogens and the hydroxyl of Thr308 in XIAP, that is not seen for Arg313 in IAP-1. Structure-based design established the [7,5]-bicycle as a suitable dipeptide replacement for the second and third amino acid positions (Figure 24).[128] Compound **53** showed potent inhibition of BIR3-IAP interactions and was cytotoxic as a single agent and in combination with doxorubicin.

A: 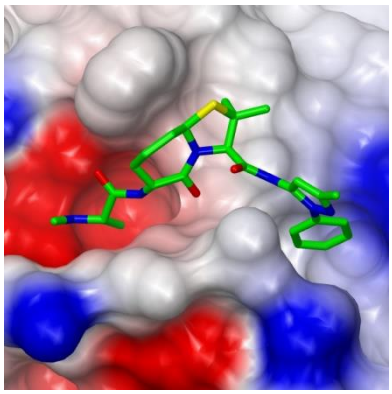 B: 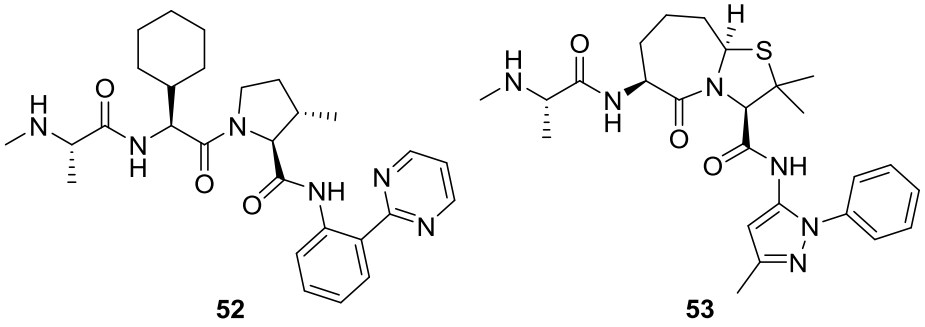

Figure 24: A: X-ray structure of the BIR3 domain of XIAP complexed to **49** (green) (pdb 2I3I); B: XIAP inhibitors **52** and **53**.

Smac mimetic AT-406 (Figure 25, **54**) incorporates a [5,8]-fused bicyclic replacement for residues 2 and 3 and is predicted to make additional hydrophobic contacts from the amide sidechain to Trp323 in the XIAP BIR3 domain.[129] AT-406 (**54**) is a pan-selective IAP inhibitor (BIR3 K_d = 4.4, 0.7, 1.9 nM XIAP, cIAP1, cIAP2, respectively), and is cytotoxic in a number of cell lines. AT-406 (**54**) shows good oral PK in a number of mammalian species.

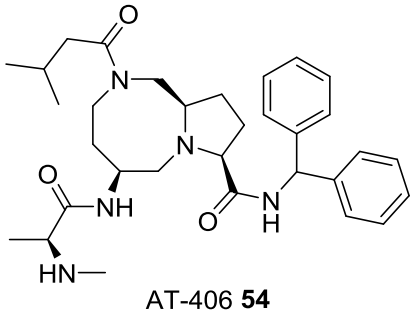

Figure 25: XIAP inhibitor AT-406 (**54**).

In order to rapidly determine the optimal substititions of tetrapeptide Smac mimetics, solid-phase peptide libraries were employed.[130] A scan of the P1-P3 positions identifed MeAla, ChGly, and Pro, for each position respectively. Similarly, a systematic scan of the P4 position showed a diphenylethylamine moieity conferred potency. Additional SAR studies at the P4 position were restricted to amines connected to an aromatic ring by one or two carbons. The thiadiazole compound GDC-0152 (**55**) showed improved potency (BIR3 K_i = 28, 17, 43 nM XIAP, cIAP1, cIAP2, respectively). The X-ray structure of **55** bound to a chimeric BIR3 domains (Figure 26) shows the thiadiazole ring positions the phenyl residue into the P4 pocket. **55** showed efficacy in a MDA-MD-231 breast cancer xenograft, and a reasonable PK profile. On the basis of these results **55** was selected for clinical trials. GDC-0917 (**56**) is a second generation IAP inhibitor which is orally active and has improved PK.[131]

A: 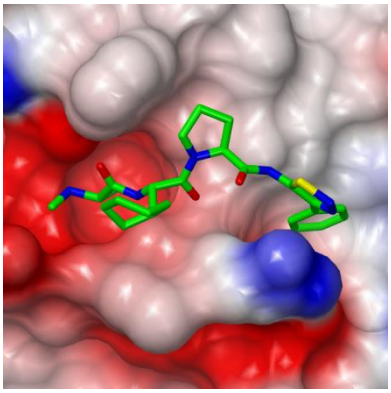 B:

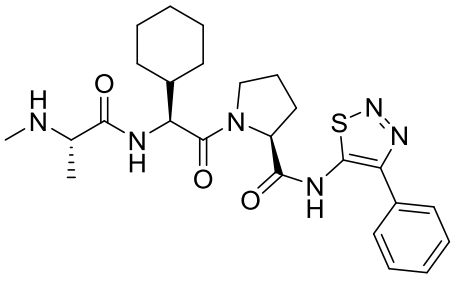

GDC-0152 **55**

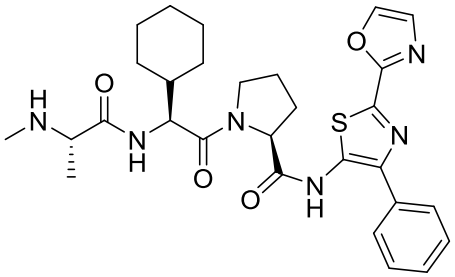

GDC-0917 **56**

Figure 26: A: X-ray structure of cIAP1/XIAP chimeric BIR3 domain with **51**; B: GDC-0152 (**55**) and GDC-0917 (**56**).

NMR and X-ray based fragment screening with XIAP-BIR3 domain identified weakly binding fragment **57**, which bound with the piperazine ring in the P1 pocket (Figure 27A) and the piperidine ring in the P3 pocket.[132] Elaboration of the fragment by the addition of a methyl group to access the alanine pocket and switching to a pyrrolidine amide gave **58** (XIAP-BIR3 IC_{50} = 52% at 1mM) (Figure 27B). Amide **55** (XIAP-BIR3 IC_{50} = 5.5 µM) was identified from a virtual screening library of amides and the *gem*-dimethyl group added to improve potency and the metabolic stability of the azaindoline. Introduction of a methoxymethyl group on the piperazine ring improved potency (**60**), and the addition of a 6-benzyl group improved interactions with the P4 pocket (**61**, XIAP-BIR3 IC_{50} = 0.16 µM). Elaboration of the piperazine substituent to an *iso*-indolinone resulted in ASTX660 (**62**) a potent inhibitor of XIAP and c-IAP1 that was selected for clinical trials.

A: 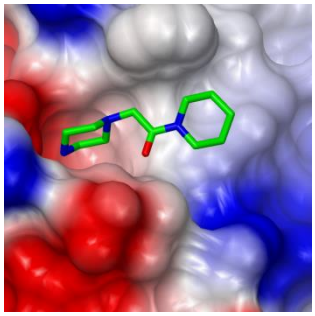 B: 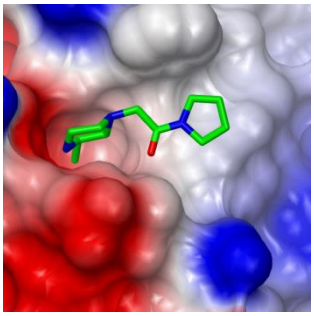 C: 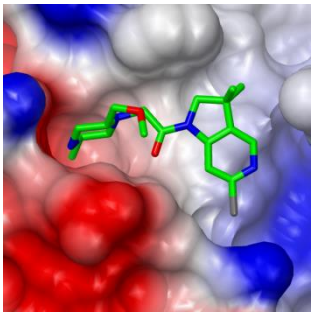 D: 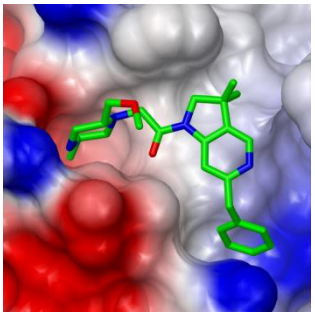

E:

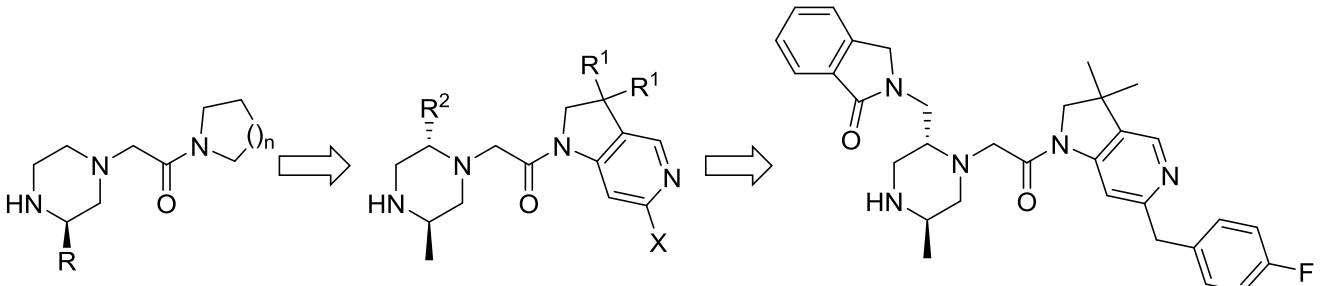

57 R = H, n = 2
58 R = CH_3, n = 1

59 R^1,R^2 = H, X = Cl
60 R^1 = CH_3, R^2= CH_2OCH_3, X = Cl
61 R^1 = CH_3, R^2 = CH_2OCH_3, X = CH_2Ph

62

Figure 27: Evolution of ASTX-660 (**58**). X-ray structure of XIAP-BIR3 (electrostatic surface, ligand green) with A: **57** (pdb 5C3H); B: **58** (pdb 5C7B); C: **60** (pdb 5C84); D: **61** (pdb 5C83); E: Evolution of ASTX660 (**62**) from **57**.

Birinapant (Figure 28, TL32711, **63**) is a bivalent Smac-mimetic that shows potent XIAP and cIAP antagonism, and induces the downregulation of specific pools of cIAPs in cells.[133,134] **63** induced apoptosis in cell lines either as a single agent by inducing the formation of a RIPK1-caspase 8 protein complex. **63** has been shown to potentiate some chemotherapy drugs in a p53-independent manner. Single-agent anti-tumour activity was demonstrated in patient derived xenograft models of ovarian cancer, colorectal cancer, and melanoma. Birinapant **63** is currently undergoing clinical trials in solid and haemaotological malignancies.

Clinical development summary

A number of XIAP and c-IAP inhibitors are in clinical trials currently in solid and haematological malignancies, as single agents and in combination with chemotherapy or anti-PD1 antibody therapies (Table 3).[135] In phase I trial GDC-0917 (**52**) was well tolerated and showed good PK and PD properties, 2/42 patients showed a complete response (one ovarian cancer and one MALT lymphoma), 4 patients had stable disease.[131,136] A phase I trial of LCL161 (Figure 28, **64**) showed the the drug was well tolerated and significant degradation of cIAP1 indicated a PD effect.[137] Although clinical evaluation of IAP inhibitors is in the early stages, initial results are encouraging.

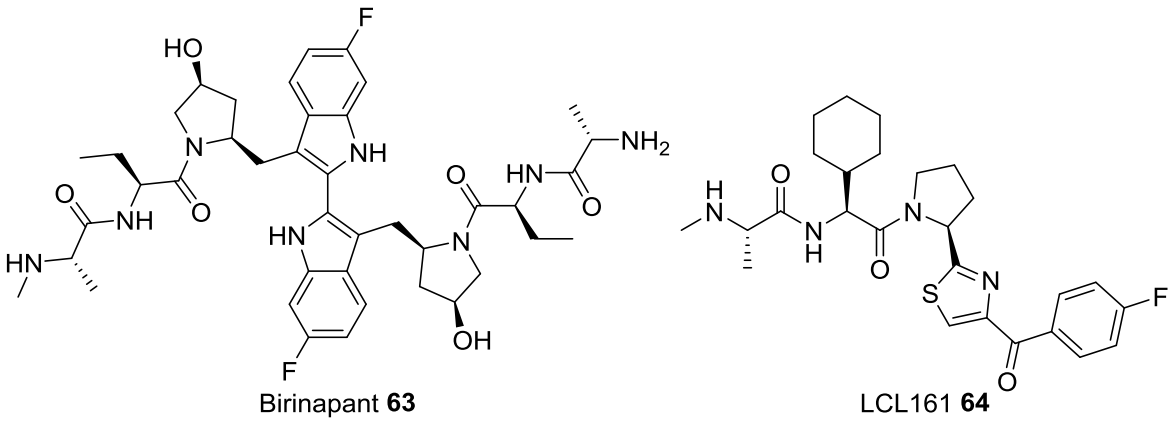

Figure 28: clinical trial candidates Birinipant (**63**) and LCL161 (**64**).

<Table 3>

Outlook and Conclusions

PPIs are a challenging class of molecular targets to address with small-molecule inhibitors. The importance of PPIs in the biology of cancer, and particularly the regulation of apoptosis, has stimulated considerable drug discovery effort. The application of modern technologies such as screening of virtual, fragment, and lead-like libraries, coupled with structure-based design has enabled the discovery of potent and selective PPI inhibitors. The inhibitors profiled in some cases stray outside the confines of the 'rule-of-five' emphasising the challenge of targeting large, lipophilic sites.[138]

The first PPI inhibitor has been licenced for clinical use in CLL, demonstrating the efficacy of selective Bcl-2 inhibition. Clinical trials of MDM2-p53 and IAP inhibitors are at an earlier stage. Preliminary results with MDM2-p53 inhibitors show promise, but with the limitations of on-target toxicity. The IAP inhibitors show less toxicity and some efficacy.

Tables

Table 1: Natural product derived PPI drugs.

Name	Compound	Structure
Vinblastine	**1**	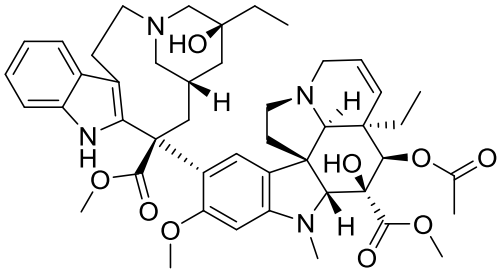
Taxol	**2**	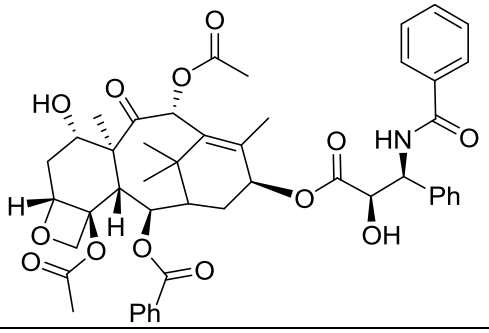
Halichondrin B	**3**	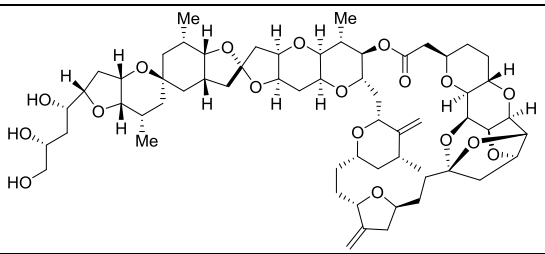
Eribulin	**4**	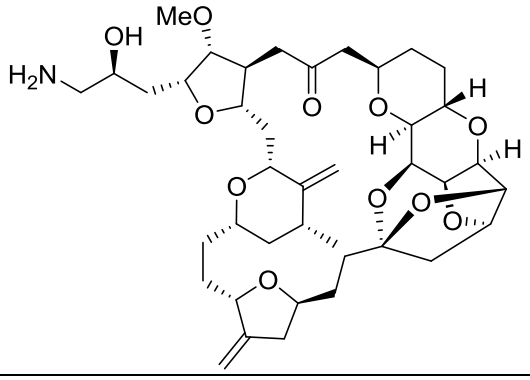
Epothilone B	**5**	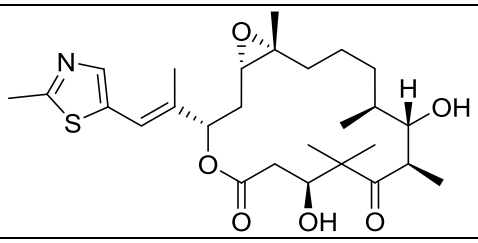

Temsirolimus	**6**	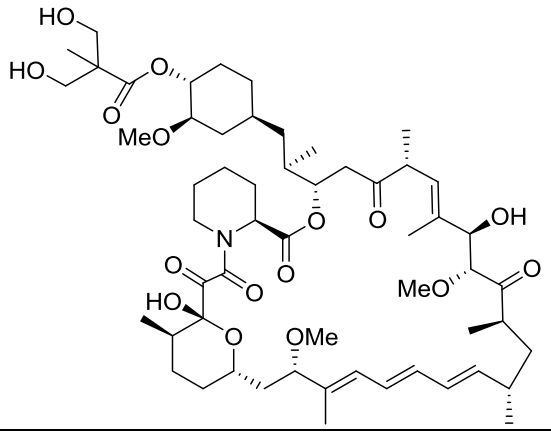

Table 2: MDM2 inhibitors in clinical trials.

Compound	Structure	Company	Clinical trial	Indications	ID	Reference
RG7112	**25**	Roche	Phase I	Liposarcoma	NCT00623870	[112–114]
Idasanutlin RG7388	**35**	Roche	Phase III	Acute myeloid leukemia	NCT02545283	[115,116]
SAR405838	**32**	Sanofi	Phase I	Liposarcoma	NCT01636479	
APG-115	**33**	Ascentage	Phase I	solid tumors, lymphomas	NCT02935907	
AMG232	**40**	Amgen	Phase I/II	Metastatic melanoma	NCT02110355	
DS-3032b	nd	Daiich-Sankyo	Phase 1 (x3)	Solid tumours, Lymphomas, Haematological, Refactory Multiple Myeloma	NCT01877382	[117]
MK-8242	nd	Merck Sharp & Dohme	Phase I	Solid tumours, AML	NCT01463696	[118,119]
CGM097	**46**	Novartis	Phase I	Solid tumours	NCT01760525	
HDM201	**48**	Novartis	Phase I/II combination with LEE011	Liposarcoma	NCT02343172	

Table 3: IAP inhibitors in clinical trials.

Compound	Structure	Company	Clinical trial	Indications	ID	Reference
AT-406	**54**	Ascenta/Debiopharm	Phase I/II	Head and neck squamous cell carcinoma – combination with chemo-radiation	NCT02022098	[129]
GDC-0152 (RG-7419)	**55**	Roche (Genentech)	Phase I	Solid cancers	NCT00977067	[130]
GDC-0917 (CUDC-427)	**56**	Curis (Genentech)	Phase I	Lymphoma and solid tumours	NCT01908413	[131,136]
ASTX660	**62**	Astex Therapeutics	Phase I/II	Lymphoma and solid tumours	NCT02503423	[132]
Birinapant (TL32711)	**63**	Tetralogic Pharma	Phase I/II	Soild tumours – combination with pembrolizumab	NCT02587962	[133,134]
AEG40826 (HGS1029)	nd	Aegera and Human Genome Sciences	Phase I	Solid tumours	NCT00708006	[139]
LCL161	**64**	Novartis	Phase II	Multiple myeloma – combination with cyclophosphamide	NCT01955434	[137]

References

1. Hanahan, D. & Weinberg, R. A. The Hallmarks of Cancer. *Cell* **100,** 57–70 (2000).

2. Gigant, B. *et al.* Structural basis for the regulation of tubulin by vinblastine. *Nature* **435,** 519–22 (2005).

3. Manfredi, J. J. & Horwitz, S. B. Taxol: an antimitotic agent with a new mechanism of action. *Pharmacol. Ther.* **25,** 83–125 (1984).

4. Cragg, G. M. Paclitaxel (Taxol): a success story with valuable lessons for natural product drug discovery and development. *Med. Res. Rev.* **18,** 315–31 (1998).

5. Amos, L. A. & Löwe, J. How Taxol® stabilises microtubule structure. *Chem. Biol.* **6,** R65–R69 (1999).

6. Towle, M. J. *et al.* In Vitro and In Vivo Anticancer Activities of Synthetic Macrocyclic Ketone Analogues of Halichondrin B. *Cancer Res.* **61,** 1013–1021 (2001).

7. Smith, J. A. *et al.* Eribulin binds at microtubule ends to a single site on tubulin to suppress dynamic instability. *Biochemistry* **49,** 1331–7 (2010).

8. Rini, B., Kar, S. & Kirkpatrick, P. Temsirolimus. *Nat. Rev. Drug Discov.* **6,** 599–600 (2007).

9. Wells, J. A. & McClendon, C. L. Reaching for high-hanging fruit in drug discovery at protein-protein interfaces. *Nature* **450,** 1001–1009 (2007).

10. Young, L., Jernigan, R. L. & Covell, D. G. A role for surface hydrophobicity in protein-protein recognition. *Protein Sci.* **3,** 717–729 (1994).

11. Clackson, T. & Wells, J. A. A hot spot of binding energy in a hormone-receptor interface. *Science (80-.).* **267,** 383–386 (1995).

12. Bogan, A. A. & Thorn, K. S. Anatomy of hot spots in protein interfaces. *J. Mol. Biol.* **280,** 1–9 (1998).

13. DeLano, W. L. Unraveling hot spots in binding interfaces: progress and challenges. *Curr. Opin. Struct. Biol.* **12,** 14–20 (2002).

14. London, N., Raveh, B. & Schueler-Furman, O. Druggable protein-protein interactions--from hot spots to hot segments. *Curr. Opin. Chem. Biol.* **17,** 952–9 (2013).

15. Overington, J. P., Al-Lazikani, B. & Hopkins, A. L. How many drug targets are there? *Nat. Rev. Drug Discov.* **5,** 993–6 (2006).

16. Laraia, L., McKenzie, G., Spring, D. R., Venkitaraman, A. R. & Huggins, D. J. Overcoming Chemical, Biological, and Computational Challenges in the Development of Inhibitors Targeting Protein-Protein Interactions. *Chem. Biol.* **22,** 689–703 (2015).

17. Cinatl, J., Speidel, D., Hardcastle, I. & Michaelis, M. Resistance acquisition to MDM2 inhibitors. *Biochem. Soc. Trans.* **42,** 752–7 (2014).

18. Gross, A., McDonnell, J. M. & Korsmeyer, S. J. BCL-2 family members and the mitochondria in apoptosis. *Genes Dev.* **13,** 1899–1911 (1999).

19. Czabotar, P. E., Lessene, G., Strasser, A. & Adams, J. M. Control of apoptosis by the BCL-2 protein family: implications for physiology and therapy. *Nat. Rev. Mol. Cell Biol.* **15,** 49–63 (2014).

20. Tsujimoto, Y., Cossman, J., Jaffe, E. & Croce, C. M. Involvement of the bcl-2 gene in human follicular lymphoma. *Science* **228,** 1440–3 (1985).

21. Beroukhim, R. *et al.* The landscape of somatic copy-number alteration across human cancers. *Nature* **463,** 899–905 (2010).

22. Garrison, S. P. *et al.* Selection against PUMA Gene Expression in Myc-Driven B-Cell Lymphomagenesis. *Mol. Cell. Biol.* **28,** 5391–5402 (2008).

23. Piazza, R. *et al.* Epigenetic Silencing of the Proapoptotic Gene BIM in Anaplastic Large Cell Lymphoma through an MeCP2/SIN3a Deacetylating Complex. *Neoplasia* **15,** 511–IN17 (2013).

24. Tagawa, H. *et al.* Genome-wide array-based CGH for mantle cell lymphoma: identification of homozygous deletions of the proapoptotic gene BIM. *Oncogene* **24,** 1348–1358 (2005).

25. Happo, L. *et al.* Maximal killing of lymphoma cells by DNA damage-inducing therapy requires not only the p53 targets Puma and Noxa, but also Bim. *Blood* **116,** 5256–5267 (2010).

26. Muchmore, S. W. *et al.* X-ray and NMR structure of human Bcl-xL, an inhibitor of programmed cell death. *Nature* **381,** 335–41 (1996).

27. Sattler, M. *et al.* Structure of Bcl-xL-Bak peptide complex: recognition between regulators of apoptosis. *Science* **275,** 983–6 (1997).

28. Yin, H. & Hamilton, A. D. Terephthalamide derivatives as mimetics of the helical region of Bak peptide target Bcl-xL protein. *Bioorg. Med. Chem. Lett.* **14,** 1375–9 (2004).

29. Gao, P. *et al.* The Bcl-2 homology domain 3 mimetic gossypol induces both Beclin 1-dependent and Beclin 1-independent cytoprotective autophagy in cancer cells. *J. Biol. Chem.* **285,** 25570–81 (2010).

30. Baell, J. B. & Holloway, G. A. New Substructure Filters for Removal of Pan Assay Interference Compounds (PAINS) from Screening Libraries and for Their Exclusion in Bioassays. *J. Med. Chem.* **53,** 2719–2740 (2010).

31. Van Poznak, C. *et al.* Oral Gossypol in the Treatment of Patients with Refractory Metastatic Breast Cancer: A Phase I/II Clinical Trial. *Breast Cancer Res. Treat.* **66,** 239–248 (2001).

32. Stein, R. C. *et al.* A preliminary clinical study of gossypol in advanced human cancer. *Cancer Chemother. Pharmacol.* **30,** 480–2 (1992).

33. Liu, G. *et al.* An Open-Label, Multicenter, Phase I/II Study of Single-Agent AT-101 in Men with Castrate-Resistant Prostate Cancer. *Clin. Cancer Res.* **15,** 3172–3176 (2009).

34. Wang, G. *et al.* Structure-Based Design of Potent Small-Molecule Inhibitors of Anti-Apoptotic Bcl-2 Proteins. *J. Med. Chem.* **49,** 6139–6142 (2006).

35. Shuker, S. B., Hajduk, P. J., Meadows, R. P. & Fesik, S. W. Discovering High-Affinity Ligands for Proteins: SAR by NMR. *Science (80-.).* **274,** 1531–1534 (1996).

36. Becattini, B. *et al.* Targeting apoptosis via chemical design: Inhibition of bid-induced cell death by small organic molecules. *Chem. Biol.* **11,** 1107–1117 (2004).

37. Oltersdorf, T. *et al.* An inhibitor of Bcl-2 family proteins induces regression of solid tumours. *Nature* **435,** 677–81 (2005).

38. Bruncko, M. *et al.* Studies leading to potent, dual inhibitors of Bcl-2 and Bcl-xL. *J. Med. Chem.* **50,** 641–62 (2007).

39. Hann, C. L. *et al.* Therapeutic efficacy of ABT-737, a selective inhibitor of BCL-2, in small cell lung cancer. *Cancer Res.* **68,** 2321–8 (2008).

40. Park, C.-M. *et al.* Discovery of an Orally Bioavailable Small Molecule Inhibitor of Prosurvival B-Cell Lymphoma 2 Proteins. *J. Med. Chem.* **51,** 6902–6915 (2008).

41. Tse, C. *et al.* ABT-263: a potent and orally bioavailable Bcl-2 family inhibitor. *Cancer Res.* **68,** 3421–8 (2008).

42. Souers, A. J. *et al.* ABT-199, a potent and selective BCL-2 inhibitor, achieves antitumor activity while sparing platelets. *Nat. Med.* **19,** 202–8 (2013).

43. Nguyen, M. *et al.* Small molecule obatoclax (GX15-070) antagonizes MCL-1 and overcomes MCL-1-mediated resistance to apoptosis. *Proc. Natl. Acad. Sci.* **104,** 19512–19517 (2007).

44. Hwang, J. J. *et al.* Phase I dose finding studies of obatoclax (GX15-070), a small molecule Pan-BCL-2 family antagonist, in patients with advanced solid tumors or lymphoma. *Clin. Cancer Res.* **16,** 4038–4045 (2010).

45. Wilson, W. H. *et al.* Navitoclax, a targeted high-affinity inhibitor of BCL-2, in lymphoid malignancies: a phase 1 dose-escalation study of safety, pharmacokinetics, pharmacodynamics, and antitumour activity. *Lancet. Oncol.* **11,** 1149–59 (2010).

46. Roberts, A. W. *et al.* Substantial Susceptibility of Chronic Lymphocytic Leukemia to BCL2 Inhibition: Results of a Phase I Study of Navitoclax in Patients With Relapsed or Refractory Disease. *J. Clin. Oncol.* **30,** 488–496 (2012).

47. Gandhi, L. *et al.* Phase I study of Navitoclax (ABT-263), a novel Bcl-2 family inhibitor, in patients with small-cell lung cancer and other solid tumors. *J. Clin. Oncol.* **29,** 909–16 (2011).

48. Rudin, C. M. *et al.* Phase II study of single-agent navitoclax (ABT-263) and biomarker correlates in patients with relapsed small cell lung cancer. *Clin. Cancer Res.* **18,** 3163–9 (2012).

49. Cang, S., Iragavarapu, C., Savooji, J., Song, Y. & Liu, D. ABT-199 (venetoclax) and BCL-2 inhibitors in clinical development. *J. Hematol. Oncol.* **8,** 129 (2015).

50. Davids, M. S. *et al.* Bcl-2 Inhibitor ABT-199 (GDC-0199) Monotherapy Shows Anti-Tumor Activity Including Complete Remissions In High-Risk Relapsed/Refractory (R/R) Chronic Lymphocytic Leukemia (CLL) and Small Lymphocytic Lymphoma (SLL). *Blood* **122,** 872–872 (2013).

51. Konopleva, M. *et al.* A Phase 2 Study of ABT-199 (GDC-0199) in Patients with Acute Myelogenous Leukemia (AML). *Blood* **124,** 118–118 (2014).

52. Roberts, A. W. *et al.* Determination of Recommended Phase 2 Dose of ABT-199 (GDC-0199) Combined with Rituximab (R) in Patients with Relapsed / Refractory (R/R) Chronic Lymphocytic Leukemia (CLL). *Blood* **124,** 325–325 (2014).

53. de Vos, S. *et al.* The BCL-2 Inhibitor ABT-199 (GDC-0199) in Combination with Bendamustine and Rituximab in Patients with Relapsed or Refractory Non-Hodgkin's Lymphoma. *Blood* **124,** 1722 (2014).

54. Stilgenbauer, S. *et al.* Venetoclax in relapsed or refractory chronic lymphocytic leukaemia with 17p deletion: a multicentre, open-label, phase 2 study. *Lancet Oncol.* **17,** 768–778 (2016).

55. O'Brien, S. M. *et al.* Phase I study of obatoclax mesylate (GX15-070), a small molecule pan-Bcl-2 family antagonist, in patients with advanced chronic lymphocytic leukemia. *Blood* **113,** 299–305 (2009).

56. Lane, D. P. Cancer. p53, guardian of the genome. *Nature* **358,** 15–16 (1992).

57. Bode, A. M. & Dong, Z. Post-translational modification of p53 in tumorigenesis. *Nat Rev Cancer* **4,** 793–805 (2004).

58. Momand, J., Wu, H.-H. & Dasgupta, G. MDM2 -- master regulator of the p53 tumor suppressor protein. *Gene* **242,** 15–29 (2000).

59. Momand, J., Zambetti, G. P., Olson, D. C., George, D. & Levine, A. The mdm-2 oncogene product forms a complex with p53 protein and inhibits p53-mediated transactivation. *Cell* **69,** 1237–1245 (1992).

60. Toledo, F. & Wahl, G. M. Regulating the p53 pathway: in vitro hypotheses, in vivo veritas. *Nat. Rev. Cancer* **6,** 909–923 (2006).

61. Uhrinova, S. *et al.* Structure of free MDM2 N-terminal domain reveals conformational adjustments that accompany p53-binding. *J. Mol. Biol.* **350,** 587–598 (2005).

62. McCoy, M. A., Gesell, J. J., Senior, M. M. & Wyss, D. F. Flexible lid to the p53-binding domain of human Mdm2: Implications for p53 regulation. *PNAS* **100,** 1645–1648 (2003).

63. Schon, O., Friedler, A., Bycroft, M., Freund, S. M. V & Fersht, A. R. Molecular Mechanism of the Interaction between MDM2 and p53. *J. Mol. Biol.* **323,** 491–501 (2002).

64. Kussie, P. H. *et al.* Structure of the MDM2 oncoprotein bound to the p53 tumor suppressor transactivation domain. *Science (80-.).* **274,** 948–953 (1996).

65. Garcia-Echeverria, C., Chene, P., Blommers, M. J. J. & Furet, P. Discovery of potent antagonists of the interaction between human double minute 2 and tumor suppressor p53. *J. Med. Chem.* **43,** 3205–3208 (2000).

66. Bernal, F. *et al.* A Stapled p53 Helix Overcomes HDMX-Mediated Suppression of p53. *Cancer Cell* **18,** 411–22 (2010).

67. Bernal, F., Tyler, A. F., Korsmeyer, S. J., Walensky, L. D. & Verdine, G. L. Reactivation of the p53 tumor suppressor pathway by a stapled p53 peptide. *J. Am. Chem. Soc.* **129,** 2456–7 (2007).

68. Baek, S. *et al.* Structure of the stapled p53 peptide bound to Mdm2. *J. Am. Chem. Soc.* **134,** 103–106 (2012).

69. Chang, Y. S. *et al.* Stapled α−helical peptide drug development: A potent dual inhibitor of MDM2 and MDMX for p53-dependent cancer therapy. *Proc. Natl. Acad. Sci. U. S. A.* **110,** E3445-54 (2013).

70. Sakurai, K., Chung, H. S. & Kahne, D. Use of a Retroinverso p53 Peptide as an Inhibitor of MDM2. *J. Am. Chem. Soc.* **126,**

16288–16289 (2004).

71. Liu, M. *et al.* D-peptide inhibitors of the p53–MDM2 interaction for targeted molecular therapy of malignant neoplasms. *Proc. Natl. Acad. Sci.* (2010). doi:10.1073/pnas.1008930107

72. Kritzer, J. a, Stephens, O. M., Guarracino, D. a, Reznik, S. K. & Schepartz, A. β-Peptides as inhibitors of protein–protein interactions. *Bioorg. Med. Chem.* **13,** 11–16 (2005).

73. Kritzer, J. A. *et al.* Miniature Protein Inhibitors of the p53-hDM2 Interaction. *ChemBioChem* **7,** 29–31 (2006).

74. Michel, J., Harker, E. A., Tirado-Rives, J., Jorgensen, W. L. & Schepartz, A. In Silico Improvement of β3-Peptide Inhibitors of p53•hDM2 and p53•hDMX. *J. Am. Chem. Soc.* **131,** 6356–6357 (2009).

75. Fasan, R. *et al.* Using a β-Hairpin To Mimic an α-Helix: Cyclic Peptidomimetic Inhibitors of the p53–HDM2 Protein–Protein Interaction. *Angew. Chemie Int. Ed.* **43,** 2109–2112 (2004).

76. Fasan, R. *et al.* Structure-Activity Studies in a Family of β-Hairpin Protein Epitope Mimetic Inhibitors of the p53-HDM2 Protein-Protein Interaction. *ChemBioChem* **7,** 515–526 (2006).

77. Hara, T., Durell, S. R., Myers, M. C. & Appella, D. H. Probing the structural requirements of peptoids that inhibit HDM2-p53 interactions. *J. Am. Chem. Soc.* **128,** 1995–2004 (2006).

78. Whitby, L. R. & Boger, D. L. Comprehensive peptidomimetic libraries targeting protein-protein interactions. *Acc. Chem. Res.* **45,** 1698–709 (2012).

79. Yin, H. *et al.* Terphenyl-based helical mimetics that disrupt the p53/HDM2 interaction. *Angew. Chemie-International Ed.* **44,** 2704–2707 (2005).

80. Campbell, F., Plante, J. P., Edwards, T. A., Warriner, S. L. & Wilson, A. J. N-alkylated oligoamide α-helical proteomimetics. *Org. Biomol. Chem.* **8,** 2344 (2010).

81. Plante, J. P. *et al.* Oligobenzamide proteomimetic inhibitors of the p53-hDM2 protein-protein interaction. *Chem. Commun.* 5091–5093 (2009). doi:10.1039/b908207g

82. Sakurai, K. & Kahne, D. Design and synthesis of functionalized trisaccharides as p53-peptide mimics. *Tetrahedron Lett.* **51,** 3724–3727 (2010).

83. Vassilev, L. T. In Vivo Activation of the p53 Pathway by Small-Molecule Antagonists of MDM2. *Science (80-.).* **303,** 844–848 (2004).

84. Vu, B. *et al.* Discovery of RG7112: A Small-Molecule MDM2 Inhibitor in Clinical Development. *ACS Med. Chem. Lett.* **4,** 466–469 (2013).

85. Miyazaki, M. *et al.* Discovery of novel dihydroimidazothiazole derivatives as p53-MDM2 protein-protein interaction inhibitors: synthesis, biological evaluation and structure-activity relationships. *Bioorg. Med. Chem. Lett.* **22,** 6338–42 (2012).

86. Miyazaki, M. *et al.* Lead optimization of novel p53-MDM2 interaction inhibitors possessing dihydroimidazothiazole scaffold. *Bioorganic Med. Chem. Lett.* **23,** 728–732 (2013).

87. Miyazaki, M. *et al.* Discovery of DS-5272 as a promising candidate: A potent and orally active p53-MDM2 interaction inhibitor. *Bioorg. Med. Chem.* **23,** 2360–7 (2015).

88. Ding, K. *et al.* Structure-Based Design of Potent Non-Peptide MDM2 Inhibitors. *J. Am. Chem. Soc.* **127,** 10130–10131 (2005).

89. Ding, K. *et al.* Structure-based design of spiro-oxindoles as potent, specific small-molecule inhibitors of the MDM2-p53 interaction. *J. Med. Chem.* **49,** 3432–5 (2006).

90. Yu, S. *et al.* Potent and Orally Active Small-Molecule Inhibitors of the MDM2−p53 Interaction. *J. Med. Chem.* **52,** 7970–7973 (2009).

91. Zhao, Y. *et al.* Diastereomeric Spirooxindoles as Highly Potent and Efficacious MDM2 Inhibitors. *J. Am. Chem. Soc.* **135,** 7223–7234 (2013).

92. Zhao, Y. *et al.* A Potent Small-Molecule Inhibitor of the MDM2–p53 Interaction (MI-888) Achieved Complete and Durable Tumor Regression in Mice. *J. Med. Chem.* **56,** 5553–5561 (2013).

93. Wang, S. *et al.* SAR405838: An optimized inhibitor of MDM2-p53 interaction that induces complete and durable tumor regression. *Cancer Res.* 5855–5865 (2014). doi:10.1158/0008-5472.CAN-14-0799

94. Aguilar, A. *et al.* Discovery of 4-((3′ *R* ,4′ *S* ,5′ *R*)-6″-Chloro-4′-(3-chloro-2-fluorophenyl)-1′-ethyl-2″-oxodispiro[cyclohexane-1,2′-pyrrolidine-3′,3″-indoline]-5′-carboxamido)bicyclo[2.2.2]octane-1-carboxylic Acid (AA-115/APG-115): A Potent and Orally. *J. Med. Chem.* acs.jmedchem.6b01665 (2017). doi:10.1021/acs.jmedchem.6b01665

95. Ding, Q. *et al.* Discovery of RG7388, a Potent and Selective p53–MDM2 Inhibitor in Clinical Development. *J. Med. Chem.* **56,** 5979–5983 (2013).

96. Ma, Y. *et al.* Substituted piperidines as HDM2 inhibitors. *Bioorg. Med. Chem. Lett.* **24,** 1026–30 (2014).

97. Pan, W. *et al. Core modification of substituted piperidines as Novel inhibitors of HDM2–p53 protein–protein interaction*. *Bioorganic & Medicinal Chemistry Letters* **24,** (2014).

98. Ma, Y. *et al.* Pivotal role of an aliphatic side chain in the development of an HDM2 inhibitor. *ACS Med. Chem. Lett.* **5,** 572–575 (2014).

99. Bogen, S. L. *et al.* Discovery of Novel 3,3-Disubstituted Piperidines as Orally Bioavailable, Potent, and Efficacious HDM2-p53 Inhibitors. *ACS Med. Chem. Lett.* **7,** acsmedchemlett.5b00472 (2016).

100. Rew, Y. *et al.* Structure-Based Design of Novel Inhibitors of the MDM2–p53 Interaction. *J. Med. Chem.* **55,** 4936–4954 (2012).

101. Sun, D. *et al.* Discovery of AMG 232, a Potent, Selective, and Orally Bioavailable MDM2–p53 Inhibitor in Clinical Development. *J. Med. Chem.* **57,** 1454–1472 (2014).

102. Yu, M. *et al.* Discovery of Potent and Simplified Piperidinone-Based Inhibitors of the MDM2–p53 Interaction. *ACS Med. Chem. Lett.* **5,** 894–899 (2014).

103. Ye, Q. *et al.* Pharmacokinetics and metabolism of AMG 232, a novel orally bioavailable inhibitor of the MDM2–p53 interaction, in rats, dogs and monkeys: in vitro–in vivo correlation. *Xenobiotica* **45,** 681–692 (2015).

104. Gonzalez, A. Z. *et al.* Novel Inhibitors of the MDM2-p53 Interaction Featuring Hydrogen Bond Acceptors as Carboxylic Acid Isosteres. *J. Med. Chem.* **57,** 2963–2988 (2014).

105. Rew, Y. *et al.* Discovery of AM-7209, a Potent and Selective 4-Amidobenzoic Acid Inhibitor of the MDM2–p53 Interaction. *J. Med. Chem.* **57,** 10499–10511 (2014).

106. Furet, P. *et al.* The central valine concept provides an entry in a new class of non peptide inhibitors of the p53-MDM2 interaction. *Bioorg. Med. Chem. Lett.* **22,** 3498–502 (2012).

107. Vaupel, A. *et al.* Tetra-substituted imidazoles as a new class of inhibitors of the p53-MDM2 interaction. *Bioorg. Med. Chem. Lett.* **24,** 2110–2114 (2014).

108. Gessier, F. *et al.* Discovery of dihydroisoquinolinone derivatives as novel inhibitors of the p53–MDM2 interaction with a distinct binding mode. *Bioorg. Med. Chem. Lett.* **25,** 3621–3625 (2015).

109. Holzer, P. *et al.* Discovery of a Dihydroisoquinolinone Derivative (NVP-CGM097): A Highly Potent and Selective MDM2 Inhibitor Undergoing Phase 1 Clinical Trials in p53wt Tumors. *J. Med. Chem.* **58,** 6348–6358 (2015).

110. Furet, P. *et al.* Discovery of a novel class of highly potent inhibitors of the p53–MDM2 interaction by structure-based design starting from a conformational argument. *Bioorg. Med. Chem. Lett.* **26,** 4837–4841 (2016).

111. Holzer, P. *et al.* Abstract 4855: Discovery of NVP-HDM201 - First disclosure of a Next-Generation Mdm2 inhibitor with superior characteristics. *Cancer Res.* **76,** (2016).

112. Ray-Coquard, I. *et al.* Effect of the MDM2 antagonist RG7112 on the P53 pathway in patients with MDM2-amplified, well-differentiated or dedifferentiated liposarcoma: an exploratory proof-of-mechanism study. *Lancet Oncol.* **13,** 1133–1140 (2012).

113. Patnaik, A. *et al.* Clinical pharmacology characterization of RG7112, an MDM2 antagonist, in patients with advanced solid tumors. *Aacr* **76,** 587–595 (2013).

114. Andreeff, M. *et al.* Results of the Phase 1 Trial of RG7112, a Small-molecule MDM2 Antagonist in Leukemia. *Clin. Cancer Res.* **22,** 1–10 (2015).

115. Yee, K. *et al.* Phase 1/1b Study of RG7388, a Potent MDM2 Antagonist, in Acute Myelogenous Leukemia (AML) Patients (Pts). *Blood* **124,** 116 (2014).

116. Siu, L. L. DT: CP and ET: Poster: Phase 1 dose escalation, food effect, and biomarker study of RG7388, a more potent second-generation MDM2 antagonist, in patients (pts) with solid tumors. in *Journal of Clinical Oncology* **32,** Abstract #2535 (2014).

117. Bauer, T. *et al.* Abstract B27: A phase I dose escalation study of the MDM2 inhibitor DS-3032b in patients with advanced solid tumors and lymphomas. *Mol. Cancer Ther.* **14,** B27–B27 (2015).

118. Wagner, A. J. *et al.* A phase I trial of the human double minute 2 (HDM2) inhibitor MK-8242 in patients (pts) with advanced solid tumors. *J. Clin. Oncol.* **33,** 10564 (2015).

119. Ravandi, F. *et al.* A phase I trial of the human double minute 2 inhibitor (MK-8242) in patients with refractory/recurrent acute myelogenous leukemia (AML). in *Journal of Clinical Oncology* **33,** 7070 (2015).

120. LaCasse, E. C. *et al.* IAP-targeted therapies for cancer. *Oncogene* **27,** 6252–75 (2008).

121. Fulda, S. & Vucic, D. Targeting IAP proteins for therapeutic intervention in cancer. *Nat. Rev. Drug Discov.* **11,** 109–124 (2012).

122. Shi, Y. *et al.* Structural basis of IAP recognition by Smac/DIABLO. *Nature* **408,** 1008–1012 (2000).

123. Fulda, S., Wick, W., Weller, M. & Debatin, K.-M. Smac agonists sensitize for Apo2L/TRAIL- or anticancer drug-induced apoptosis and induce regression of malignant glioma in vivo. *Nat. Med.* **8,** 808–815 (2002).

124. Oost, T. K. *et al.* Discovery of potent antagonists of the antiapoptotic protein XIAP for the treatment of cancer. *J. Med. Chem.* **47,** 4417–4426 (2004).

125. Sharma, S. K., Straub, C. & Zawel, L. Development of peptidomimetics targeting IAPs. *Int. J. Pept. Res. Ther.* **12,** 21–32 (2006).

126. González-Lpez, M. *et al.* Design, synthesis and evaluation of monovalent Smac mimetics that bind to the BIR2 domain of the anti-apoptotic protein XIAP. *Bioorganic Med. Chem. Lett.* **21,** 4332–4336 (2011).

127. Ndubaku, C. *et al.* Antagonism of c-IAP and XIAP proteins is required for efficient induction of cell death by small-molecule IAP antagonists. *ACS Chem. Biol.* **4,** 557–566 (2009).

128. Zobel, K. *et al.* Design, synthesis, and biological activity of a potent Smac mimetic that sensitizes cancer cells to apoptosis by antagonizing IAPs. *ACS Chem. Biol.* **1,** 525–533 (2006).

129. Cai, Q. *et al.* A potent and orally active antagonist (SM-406/AT-406) of multiple inhibitor of apoptosis proteins (IAPs) in clinical development for cancer treatment. *J. Med. Chem.* **54,** 2714–26 (2011).

130. Flygare, J. A. *et al.* Discovery of a Potent Small-Molecule Antagonist of Inhibitor of Apoptosis (IAP) Proteins and Clinical Candidate for the Treatment of Cancer (GDC-0152). *J. Med. Chem.* **55,** 4101–4113 (2012).

131. Wong, H. *et al.* Learning and Confirming with Preclinical Studies: Modeling and Simulation in the Discovery of GDC-0917, an Inhibitor of Apoptosis Proteins Antagonist. *Drug Metab. Dispos.* **41,** 2104–2113 (2013).

132. Chessari, G. *et al.* Fragment-Based Drug Discovery Targeting Inhibitor of Apoptosis Proteins: Discovery of a Non-Alanine Lead Series with Dual Activity Against cIAP1 and XIAP. *J. Med. Chem.* **58,** 6574–6588 (2015).

133. Allensworth, J. L., Sauer, S. J., Lyerly, H. K., Morse, M. A. & Devi, G. R. Smac mimetic Birinapant induces apoptosis and enhances TRAIL potency in inflammatory breast cancer cells in an IAP-dependent and TNF-α-independent mechanism. *Breast Cancer Res. Treat.* **137,** 359–71 (2013).

134. Benetatos, C. A. *et al.* Birinapant (TL32711), a bivalent SMAC mimetic, targets TRAF2-associated cIAPs, abrogates TNF-

induced NF-κB activation, and is active in patient-derived xenograft models. *Mol. Cancer Ther.* **13,** 867–79 (2014).

135. Hird, A. W., Aquila, B. M., Hennessy, E. J., Vasbinder, M. M. & Yang, B. Small molecule inhibitor of apoptosis proteins antagonists: a patent review. *Expert Opin. Ther. Pat.* **1,** 1–20 (2015).

136. Tolcher, A. W. *et al.* Phase I study of safety and pharmacokinetics (PK) of GDC-0917, an antagonist of inhibitor of apoptosis (IAP) proteins in patients (Pts) with refractory solid tumors or lymphoma. | 2013 ASCO Annual Meeting | Abstracts | Meeting Library. in *Journal of Clinical Oncology* **31,** 2503 (2013).

137. Weisberg, E. *et al.* Smac mimetics: implications for enhancement of targeted therapies in leukemia. *Leukemia* **24,** 2100–9 (2010).

138. Lipinski, C. A., Lombardo, F., Dominy, B. W. & Feeney, P. J. Experimental and computational approaches to estimate solubility and permeability in drug discovery and development settings. *Adv. Drug Deliv. Rev.* **46,** 3–26 (2001).

139. Sikic, B. I. *et al.* Safety, pharmacokinetics (PK), and pharmacodynamics (PD) of HGS1029, an inhibitor of apoptosis protein (IAP) inhibitor, in patients (Pts) with advanced solid tumors: Results of a phase I study. in *Journal of Clinical Oncology* **29,** 3008 (2011).